PERGAMON

International Journal of Multiphase Flow 27 (2001) 299–345

International Journal of Multiphase Flow

www.elsevier.com/locate/ijmulflow

Stability of rapidly evaporating droplets and liquid shells

M. Shusser*, [1], D. Weihs

Faculty of Aerospace Engineering, Technion — Israel Institute of Technology, Haifa 32000, Israel

Received 25 March 1999; received in revised form 17 February 2000

Abstract

The paper presents a study of stability of rapidly evaporating droplets and liquid shells occurring in the process of explosive boiling, where, in addition to surface evaporation, a vapor bubble grows within a highly superheated liquid droplet immersed in a liquid or gas medium. To get better insight into the problem, two simpler but related problems are studied before the full stability problem is treated. First, the stability of an evaporating, highly superheated liquid droplet is analyzed, in order to estimate the influence of the outer evaporation from the droplet surface. The linear stability of the process at the final stages of explosive boiling, when the droplet forms an expanding liquid shell, is studied next. Finally, the general case of explosive boiling stability is considered. It is shown that the process is unstable, as indeed has been found in existing experiments. © 2001 Elsevier Science Ltd. All rights reserved.

Keywords: Explosive boiling; Stability; Bubble; Droplet; Evaporation

1. Introduction

Explosive boiling is a process of rapid phase transition from liquid to vapor, which occurs when the liquid is highly superheated (Avedisian, 1985; Shepherd and Sturtevant, 1982; Reid, 1983). The process is characterized by very high evaporation rates, formation of an internal bubble and deviation from thermodynamic equilibrium. It usually occurs so fast (100–200 μs at atmospheric pressure) that it resembles an explosion.

* Corresponding author.
[1] Pressent address: Graduate Aeronautical Laboratories, California Institute of Technology, Pasadena, CA 91125, USA.

PII: S0301-9322(00)00017-3

Explosive boiling occurs when liquid droplets are suddenly and massively heated, say by immersion in a hot medium, by laser heating (Chitavnis, 1987) or by passage through a shock wave (Frost, 1989). It is also obtained by sudden decompression, as in liquids ejected in space (Fuchs and Legge, 1979; Miller, 1985).

One of the most interesting features of explosive boiling is the very high evaporation rate attainable in this process. One cause of such strong evaporation is thought to be the significant increase in the area of the evaporation surface caused by instability of the bubble interface (Avedisian, 1985; Shepherd and Sturtevant, 1982; McCann et al., 1989). This instability, first observed by Shepherd and Sturtevant (1982), manifests itself as wrinkling and roughening of the vapor bubble surface followed by its distortion. The increased area of the evaporation surface provides the necessary heat transfer to support explosive boiling.

Recently Shusser and Weihs (1999) proposed a mathematical model describing growth of an internal vapor bubble produced by homogeneous nucleation within a liquid droplet during explosive boiling. The predictions of the model were confirmed by existing experimental results for explosive boiling of superheated droplets (Shepherd and Sturtevant, 1982; McCann et al., 1989). The instability of explosive vapor bubble growth was not, however, considered by Shusser and Weihs (1999). Proper understanding of this instability may throw light on the physics of explosive boiling.

Explosive boiling instability is related to the instability of laminar flames discovered by Landau (1944) and investigated for spherical flames by Istratov and Librovich (1969). It is also connected to the instability of evaporation surfaces (Miller, 1973; Palmer, 1976; Prosperetti and Plesset, 1984) and to the problem of spherical bubble stability (Birkhoff, 1954, 1956; Plesset, 1954; Plesset and Mitchell, 1956). The unperturbed state is time-dependent (growth of a spherical vapor bubble within a liquid droplet) and hence normal-mode analysis is not appropriate.

Instabilities developing on the outer surface of the liquid droplet can be capillary instability if the droplet is situated in a liquid medium or evaporating surface instability if the medium is gaseous. To analyze the interaction of the process on both interfaces one must consider two types of perturbations which we shall call "symmetric" and "antisymmetric" in analogy with the stability of liquid films (Squire, 1953) or annular liquid jets (Meyer and Weihs, 1987).

The physical mechanism responsible for this instability is not fully understood at present. Sturtevant and Shepherd (1982) used the Landau theory to estimate stability limits and growth rates for explosive boiling. Recently Lee and Merte (1998) showed that approximating the evaporation surface as a plane and using instantaneous information for a growing spherical vapor bubble, one can reasonably predict the occurrence of instability and its wavelength. Nevertheless, an understanding of rapid evaporation instability for the *spherical* case has not been achieved yet (Lee and Merte, 1998).

Our aim is to investigate the linear stability of explosive boiling of a liquid droplet in liquid or gas medium. We concentrate on hydrodynamic aspects of the problem but consider spherical geometry and include both interfaces into the analysis. We start by studying two simpler but related problems before treating the general case.

The plan of the present paper is as follows. In the next section, the stability of evaporation of a highly superheated liquid droplet is studied. Section 3 deals with the problem of linear stability of a thin expanding liquid spherical shell. Then we proceed to analyze the general case of explosive boiling stability in Section 4.

2. Stability of a highly superheated evaporating liquid droplet

2.1. Statement of the problem

Take a spherical, highly superheated liquid droplet surrounded by vapor of the same composition. The droplet evaporates, creating vapor flow in the host medium, as shown in Fig. 1. Here no internal vapor bubbles are produced. Our purpose is to study the linear stability of this process.

The stability of evaporation has been investigated only for evaporation from plane surfaces (Miller, 1973; Palmer, 1976; Prosperetti and Plesset, 1984; Higuera, 1987). Moreover, most of the work has been devoted to studying marginal stability, which may be inappropriate for investigation of the stability of evaporation (Prosperetti and Plesset, 1984, p. 1590). Therefore, as a first stage in the study of the stability of an explosively evaporating droplet, we make several simplifying assumptions based on the observations of high superheating and very strong evaporation. These assumptions are consistent with explosive boiling.

We assume that:

1. The vapor and the liquid are inviscid, incompressible fluids.
2. Evaporation rate in the base flow is constant.
3. The flow perturbations do not influence the evaporation rate.
4. The flow field is spherically symmetric.

Shepherd and Sturtevant (1982) observed, for evaporation into the interior of a bubble, that typical velocities for explosive boiling are about 15 m/s. At such velocities, density variations due to pressure variations are small, as the Mach number is much less than one. In the absence of quantitative data for outer evaporation from the surface of a droplet boiling explosively, we assume that this remains true in our case. Influence of temperature variations on density variations was estimated by Prosperetti and Plesset (1984) and found negligible. They have also demonstrated that viscosity can be neglected.

Experimentally, it was found for explosive evaporation into a bubble, that evaporation rate remains approximately constant (Shepherd and Sturtevant, 1982). Due to high superheating, the evaporation rate value is close to its kinetic theory limit (Shusser and Weihs, 1999). Under these conditions the influence of pressure and temperature changes on the evaporation rate is relatively limited (Ytrehus, 1997, Fig. 12). Hence, we consider the problem of steady evaporation and assume that the evaporation rate in the base flow is constant. The same approach was chosen by Prosperetti and Plesset (1984) in their analysis of stability of a plane evaporating surface. Calculating the temperature field inside the droplet for the base flow (see Appendix A) one can demonstrate that this approximation is indeed reasonable.

Estimation of the droplet surface temperature perturbation (see Appendix A) shows that the temperature perturbation is much smaller than any change in the surface temperature itself and therefore it can be neglected. It should be emphasized that though the evaporation rate (mass of evaporated liquid from unit area of the interface per unit time) remains approximately constant, the overall evaporating mass flux can increase significantly due to increase in the area of the interface.

The assumption of spherical symmetry is discussed by Avedisian (1985) and Shusser and Weihs (1999).

2.2. The unperturbed (base) flow

Let u_+, p_+ and u_-, p_- be the velocity and the pressure in the vapor and liquid phase, respectively. p_0 is the pressure far from the droplet, J is the evaporation rate (per unit surface area), $R = R(t)$ is the droplet radius where $R_0 = R(0)$ and ρ, ρ_v are the densities of the liquid

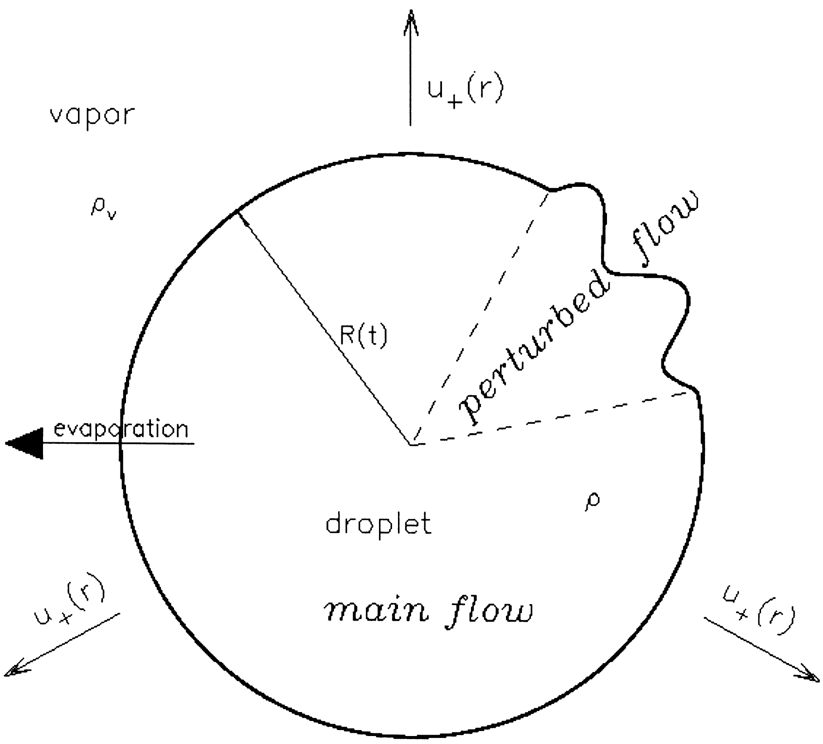

Fig. 1. A highly superheated evaporating droplet.

and the vapor, respectively; $\alpha = \rho_v/\rho$ $(0 < \alpha < 1)$. Furthermore σ is the surface tension; r is the radial coordinate in the spherical coordinates (r, θ, φ); t is the time.

For spherical incompressible flow with constant evaporation rate to satisfy the conservation of mass, the droplet radius must decrease linearly with time

$$R = R_0 - \frac{J}{\rho} t \tag{1}$$

From the conservation of mass and momentum at the interface

$$\rho_v \left(u_+|_{r=R} - \frac{\mathrm{d}R}{\mathrm{d}t} \right) = J \tag{2}$$

$$\rho \left(u_-|_{r=R} - \frac{\mathrm{d}R}{\mathrm{d}t} \right) = J \tag{3}$$

$$-\rho \left(u_-|_{r=R} - \frac{\mathrm{d}R}{\mathrm{d}t} \right) u_-|_{r=R} + \rho_v \left(u_+|_{r=R} - \frac{\mathrm{d}R}{\mathrm{d}t} \right) u_+|_{r=R} = p_-|_{r=R} - p_+|_{r=R} - \frac{2\sigma}{R} \tag{4}$$

one obtains that the velocity inside the droplet vanishes and the pressure there is uniform but time-dependent.

$$u_- \equiv 0 \tag{5}$$

$$p_- = p_0 - \frac{J^2}{2\rho}(1-\alpha)\left(3 - \frac{1}{\alpha}\right) + \frac{2\sigma}{R(t)} \tag{6}$$

while the velocity and the pressure in the vapor are given by

$$u_+ = \frac{J}{\rho}\left(\frac{1}{\alpha} - 1\right)\frac{R^2}{r^2} \tag{7}$$

$$p_+ = p_0 - \frac{J^2}{2\rho}(1-\alpha)\frac{R}{r}\left[4 + \left(\frac{1}{\alpha} - 1\right)\frac{R^3}{r^3}\right] \tag{8}$$

2.3. Boundary conditions in the perturbed flow

The droplet is now assumed to have the following surface shape

$$r = R(t) + \varepsilon(\theta;\varphi;t) \tag{9}$$

where $\varepsilon \ll R$ (see insert in Fig. 1).

We denote the components of perturbation velocity in spherical coordinates and perturbation of pressure v'_{r-}, $v'_{\theta-}$, $v'_{\varphi-}$, p'_{-} in the droplet and v'_{r+}, $v'_{\theta+}$, $v'_{\varphi+}$, p'_{+} in the vapor. At the interface they satisfy boundary conditions which are the conservation of mass, the constancy of the evaporation rate and the conservation of the three components of momentum.

Istratov and Librovich (1969) solved a similar (but inverse) problem of spherical flame stability. Following their solution we obtain that at the unperturbed surface of the droplet $r = R(t)$

$$v_{r'-} = \frac{\partial \varepsilon}{\partial t} \tag{10}$$

$$v_{r'+} + \varepsilon \frac{\mathrm{d}u_+}{\mathrm{d}r} = \frac{\partial \varepsilon}{\partial t} \tag{11}$$

$$v'_{\theta-} = v'_{\theta+} + \frac{1}{R}\frac{\partial \varepsilon}{\partial \theta} u_+ \tag{12}$$

$$v'_{\varphi-} = v'_{\varphi+} + \frac{1}{R \sin\theta}\frac{\partial \varepsilon}{\partial \varphi} u_+ \tag{13}$$

$$p'_{-} = p'_{+} + \varepsilon \frac{\mathrm{d}p_+}{\mathrm{d}r} + \sigma\left(\Lambda - \frac{2}{R}\right) \tag{14}$$

where Λ is the perturbed droplet surface curvature.

2.4. Perturbed flow

For inviscid fluid, the flow inside the perturbed droplet remains irrotational. Defining the perturbation potential Φ'_{-} and choosing an appropriate solution of the Laplace equation

$$\Phi'_{-} = f(t) r^n Y_n^m(\theta;\varphi) \tag{15}$$

where Y_n^m are spherical harmonics, one obtains the components of perturbation velocity and perturbation pressure

$$v'_{r-} = nfr^{n-1} Y_n^m; \quad v'_{\theta-} = fr^{n-1}\frac{\partial Y_n^m}{\partial \theta}; \quad v'_{\varphi-} = fr^{n-1}\frac{1}{\sin\theta}\frac{\partial Y_n^m}{\partial \varphi} \tag{16}$$

$$p'_{-} = -\rho \frac{\mathrm{d}f}{\mathrm{d}t} r^n Y_n^m \tag{17}$$

The flow in the vapor phase will be rotational due to the creation of vorticity at the distorted surface of the perturbed droplet. It should be stressed that it is not possible to use the Laplace equation for pressure perturbations in the vapor phase (Landau, 1944; Istratov and Librovich, 1969) because there is a vapor flow in the unperturbed case. It turns out that our problem (outer evaporation from the droplet surface) is much more difficult than the problem of Istratov and Librovich (1969) (expansion of spherical flame) or the problem of evaporation into an inner bubble.

Due to the velocity perturbation $\boldsymbol{v}'_+$ being solenoidal, we can divide it into toroidal and poloidal parts $\boldsymbol{T}, \boldsymbol{S}$ (Chandrasekhar, 1961, p. 225)

$$\boldsymbol{v}'_+ = \boldsymbol{T} + \boldsymbol{S} \tag{18}$$

where

$$T_r = 0; \qquad T_\theta = \frac{T(r)}{r\sin\theta}\frac{\partial Y_n^m}{\partial\varphi}; \qquad T_\varphi = -\frac{T(r)}{r}\frac{\partial Y_n^m}{\partial\theta} \tag{19}$$

$$S_r = \frac{n(n+1)}{r^2}S(r)Y_n^m; \qquad S_\theta = \frac{1}{r}\frac{\partial S}{\partial r}\frac{\partial Y_n^m}{\partial\theta}; \qquad S_\varphi = \frac{1}{r\sin\theta}\frac{\partial S}{\partial r}\frac{\partial Y_n^m}{\partial\varphi} \tag{20}$$

The vorticity $\boldsymbol{\Omega}$ can also be divided

$$\boldsymbol{\Omega} = \tilde{\boldsymbol{T}} + \tilde{\boldsymbol{S}} \tag{21}$$

where the functions $\tilde{T}, \tilde{S}$ satisfy (Chandrasekhar, 1961, p. 226)

$$\tilde{T} = \frac{n(n+1)}{r^2}S - \frac{\mathrm{d}^2 S}{\mathrm{d}r^2} \tag{22}$$

$$\tilde{S} = T \tag{23}$$

The radial component of vorticity is

$$\Omega_r = \frac{n(n+1)}{r^2}T(r)Y_n^m \tag{24}$$

We now show that in the linear approximation Ω_r vanishes.

Indeed, linearizing the vorticity equation for inviscid flow we obtain for Ω_r

$$\frac{\partial\Omega_r}{\partial t} + u_+\frac{\partial\Omega_r}{\partial r} - \Omega_r\frac{\mathrm{d}u_+}{\mathrm{d}r} = 0 \tag{25}$$

and therefore Ω_r is not identically zero only if it is created at the perturbed interface (9). On the other hand, the vorticity is of order $O(\varepsilon)$ and therefore, neglecting second-order terms, one can calculate it at the surface of the unperturbed droplet $r = R$. Then using the definition of vorticity and boundary conditions (12) and (13) one obtains that the radial component of vorticity is continuous at the interface. It is zero inside the droplet, so that it must vanish in the vapor too.

We have therefore obtained that Ω_r is a second-order quantity and hence negligible in the investigation of linear stability. Thus, we put

$$T(r) \equiv 0 \tag{26}$$

That is, in the vapor phase the flow-field has only a poloidal part and the vorticity field has only a toroidal part. This is in accordance with Prosperetti (1977, p. 344) who stated that in perturbed spherical flows a poloidal part of the vorticity cannot be generated if it vanishes at the initial moment.

Returning to the calculation of the velocity field within the vapor, relation (22) is now an ordinary differential equation, with general solution

$$S = \frac{C(t)}{r^n} + D(t)r^{n+1} + S_p \tag{27}$$

where S_p is the particular solution.

We assume that when $r \to \infty$ the vorticity tends to zero sufficiently rapidly so that $S_p \to 0$ too. Then

$$D(t) \equiv 0 \tag{28}$$

We are interested in the behavior of $S(r;\, t)$ near the droplet surface. Therefore we approximate $\tilde{T}(r;\, t)$ by its value at the droplet surface, which we call $F(t)$

$$\tilde{T}(r;\, t) \approx \tilde{T}(R(t);\, t) \equiv F(t) \tag{29}$$

Substituting Eq. (29) into Eq. (22) and using the resultant ordinary differential equation to calculate S_p, we obtain the following approximate solution for S:

$$S = \frac{C(t)}{r^n} + \frac{F(t)r^2}{n(n+1)-2} \tag{30}$$

The solution (30) always exists, as we are interested in the perturbation modes for which $n \geq 2$. The fact that it does not satisfy the condition at infinity is not relevant as we use it only near the droplet surface.

From Eqs. (18), (20), (26) and (30) one obtains that the surface values of the perturbed velocity field in the vapor are

$$v'_{r+} = \left(\frac{n(n+1)C}{R^{n+2}} + \frac{n(n+1)F}{n(n+1)-2} \right) Y_n^m \tag{31}$$

$$v'_{\theta+} = \left(-\frac{nC}{R^{n+2}} + \frac{2F}{n(n+1)-2} \right) \frac{\partial Y_n^m}{\partial \theta} \tag{32}$$

$$v'_{\varphi+} = \left(-\frac{nC}{R^{n+2}} + \frac{2F}{n(n+1)-2} \right) \frac{1}{\sin\theta} \frac{\partial Y_n^m}{\partial \varphi} \tag{33}$$

The pressure perturbation is calculated from the linearized Euler equation. The result for $r = R$ is

$$\frac{p'_+}{\rho_v} = \left[\frac{n}{R^{n+1}} \frac{dC}{dt} - \frac{2R}{n(n+1)-2} \frac{dF}{dt} - \frac{J}{\rho} \left(\frac{1}{\alpha} - 1 \right) \left(\frac{n(n+1)C}{R^{n+2}} + \frac{2F}{n(n+1)-2} \right) \right] Y_n^m \tag{34}$$

In addition, the droplet surface distortion is

$$\varepsilon = a_1(t) Y_n^m(\theta\ \varphi); \quad n > 2 \tag{35}$$

2.5. Stability analysis

Substituting Eqs. (16), (17), (31)–(34) into the boundary conditions (10)–(14) and denoting

$$a_2(t) = f(t) R^{n-1}; \qquad a_3(t) = \frac{C(t)}{R^{n+2}}; \qquad a_4(t) = \frac{F(t)}{n(n+1)-2} \tag{36}$$

we obtain the following system of equations for the functions a_1, a_2, a_3, a_4

$$n a_2 = \frac{da_1}{dt} \tag{37}$$

$$n(n+1)(a_3 + a_4) - \frac{2}{R} \frac{J}{\rho} \left(\frac{1}{\alpha} - 1 \right) a_1 = \frac{da_1}{dt} \tag{38}$$

$$a_2 = -n a_3 + 2 a_4 + \frac{J}{\rho} \left(\frac{1}{\alpha} - 1 \right) \frac{a_1}{R} \tag{39}$$

$$\begin{aligned} &-\left(R \frac{da_2}{dt} + (n\text{-}1) \frac{J}{\rho} a_2 \right) \\ &\quad = \alpha n \left(R \frac{da_3}{dt} - \frac{J}{\rho} \left(1 + \frac{n+1}{\alpha} \right) a_3 \right) - 2\alpha \left(R \frac{da_4}{dt} + \frac{J}{\rho} \left(\frac{1}{\alpha} - 1 \right) a_4 \right) + \frac{2J^2}{\rho^2} \left(\frac{1}{\alpha} - 1 \right) \frac{a_1}{R} \\ &\qquad + \frac{\sigma(n-1)(n+2)}{\rho R^2} a_1 \end{aligned} \tag{40}$$

from which the equation for the amplitude of the droplet surface perturbation $a_1(t)$ is obtained, as

$$\frac{R}{n}(1-\alpha)\frac{d^2a_1}{dt^2}+\frac{(n-1)}{n}\left(3-\frac{1}{n+1}+\alpha\right)\frac{J}{\rho}\frac{da_1}{dt}$$
$$+\left(-\left(\frac{1}{\alpha}-1\right)\frac{(n-1)^2}{n+1}+\frac{\sigma\rho(n-1)(n+2)}{J^2R}\right)\frac{J^2}{\rho^2}\frac{a_1}{R}=0 \tag{41}$$

Taking the unperturbed droplet radius R as an independent variable we re-write Eq. (41) as

$$R\frac{d^2a_1}{dR^2}-\beta\frac{da_1}{dR}+\left(-\frac{\gamma}{R}+\frac{\delta}{R^2}\right)a_1=0 \tag{42}$$

where

$$\beta=\frac{(n-1)}{1-\alpha}\left(3-\frac{1}{n+1}+\alpha;\right)\quad \gamma=\frac{1}{\alpha}\frac{n(n-1)^2}{n+1};\quad \delta=\frac{\sigma\rho}{J^2}\frac{n(n-1)(n+2)}{1-\alpha} \tag{43}$$

Choosing

$$x=2\sqrt{\frac{\delta}{R}};\qquad y=x^{\beta+1}a_1 \tag{44}$$

we retrieve a Bessel equation

$$\frac{d^2y}{dx^2}+\frac{1}{x}\frac{dy}{dx}+\left[1-\frac{\left(4\gamma+(\beta+1)^2\right)}{x^2}\right]y=0 \tag{45}$$

Therefore the general solution of Eq. (42) is

$$a_1=R^{\frac{\beta+1}{2}}\left[C_1\ J_v\left(2\sqrt{\frac{\delta}{R}}\right)+C_2Y_v\left(2\sqrt{\frac{\delta}{R}}\right)\right] \tag{46}$$

where

$$v=\sqrt{4\gamma+(\beta+1)^2} \tag{47}$$

Hence when $R\rightarrow 0$

$$\frac{a_1}{R}\sim R^{\frac{2\beta-1}{4}} \tag{48}$$

One sees that $\beta>8/3$ when $n\geq 2$ and $0<\alpha<1$ and therefore $a_1/R\rightarrow 0$ when $R\rightarrow 0$, i.e., droplet surface perturbations tend to zero faster than the droplet radius. The solution is thus stable.

A question arises about the validity of this analysis, due to the assumption of $\frac{\varepsilon}{R}\ll 1$ (Eq. (9)) which is only justified a posteriori here.

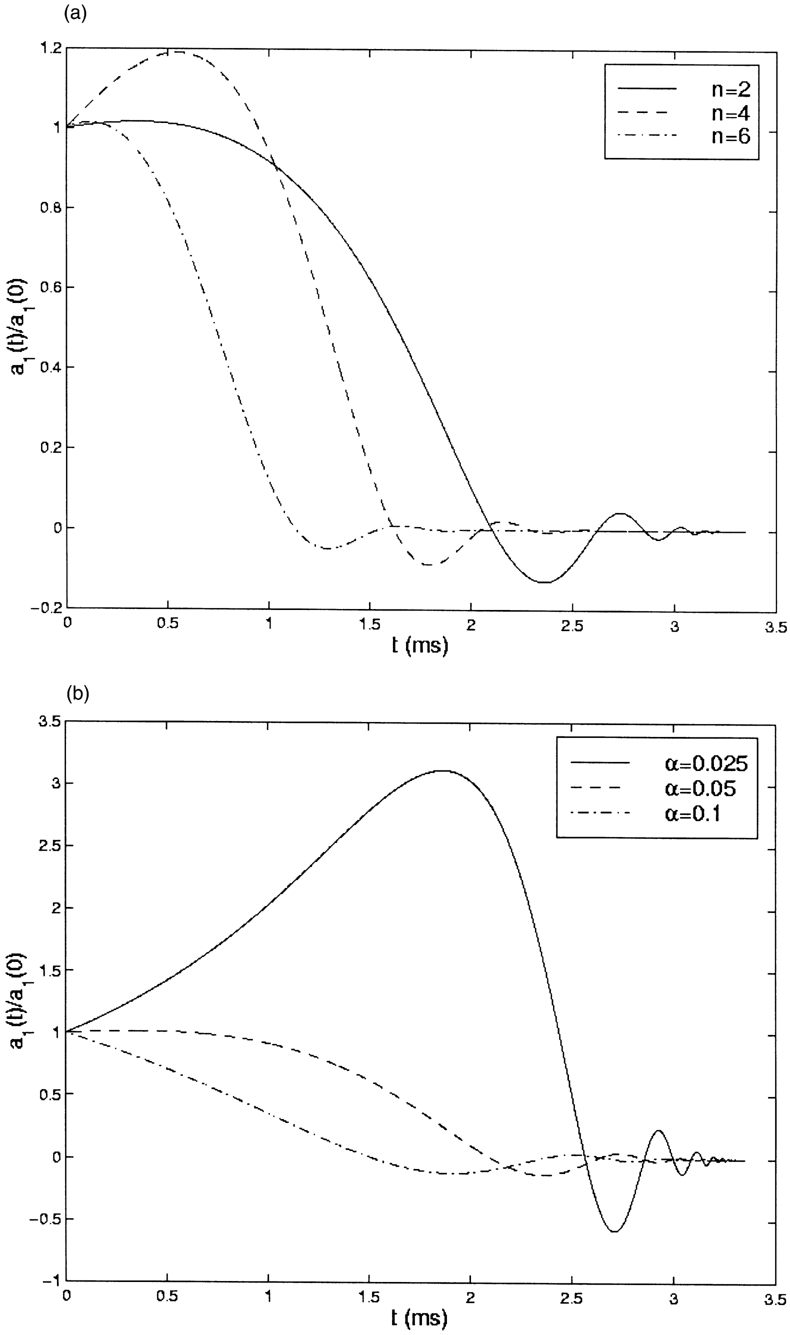

Fig. 2. Time evolution of droplet surface shape perturbation for explosive boiling of a water droplet: (a) $\alpha = 0.05$; $n = 2$; 4; 6; (b) $n = 2$; $\alpha = 0.025$; 0.05; 0.1. a_1, n are defined in Eq. (35) and $\alpha = \rho_v/\rho$.

However, returning to our main objective, stability of explosive boiling, the results of this section suggest, at least as a first step in studying the problem, to ignore the outer evaporation from the droplet surface when analyzing the stability of a liquid droplet boiling explosively, as R never tends to zero in the full problem where an internal vapor bubble is produced.

To illustrate the time evolution of the perturbation amplitude $a_1(t)$, we calculated it for explosive boiling of a water droplet of a diameter of one mm. The relevant physical properties of water at the superheat limit are as follows (Shusser, 1997): density $\rho = 665$ kg/m^3, surface tension $\sigma = 0.0128$ N/m, evaporative mass flux $J = 99.3$ kg/(m^{2}s). (Shepherd and Sturtevant, 1982, p. 393) observed that for evaporation into a bubble the vapor density during explosive boiling can be as high as 35% of the liquid density. Though in an unconfined flow the vapor density would not be so high, we considered relatively high values of vapor to liquid density ratio α.

Fig. 2(a) shows the time dependence of the normalized perturbation amplitude $a_1(t)/a_1(0)$ for $\alpha = 0.05$ and three wave numbers $n = 2, 4, 6$. In Fig. 2b we plotted $a_1(t)/a_1(0)$ for $n = 2$ and $\alpha = 0.025, 0.05, 0.1$. One sees that the decay is faster for higher wave numbers and when vapor and liquid densities are closer in value ($\alpha \to 1$), as can also be seen from Eq. (43).

Defining characteristic times for the basic flow τ_R and for the perturbation τ_a as the leading order terms in $R/\dot{R}$ and $a_1/(\mathrm{d}a_1/\mathrm{d}t)$, one obtains that $\tau_R = R_0\rho/J$ and $\tau_a = 4\tau_R/(2\beta + 3)$. This means that τ_a is at least twice as small as τ_R, i.e. the perturbations do have enough time to

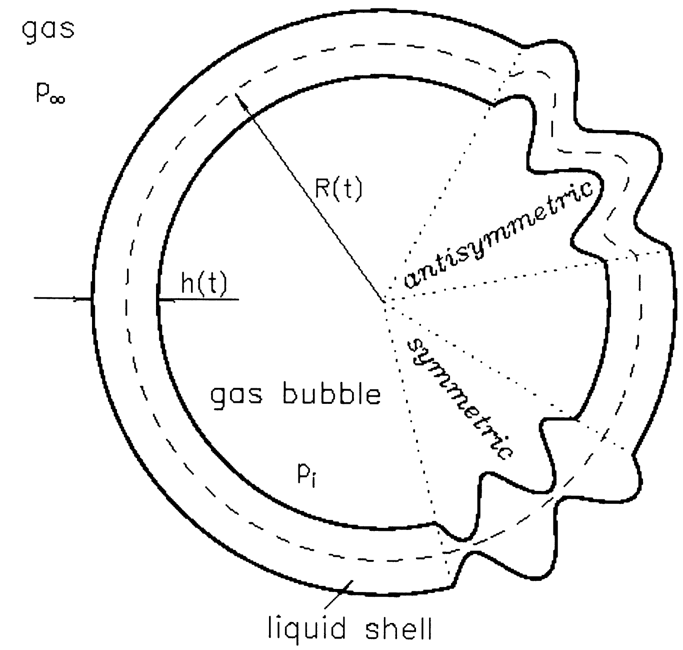

Fig. 3. A thin expanding liquid shell.

decay during the droplet evaporation. For given density ratio α, τ_R is smaller for larger values of n, in accordance with the already mentioned fact of faster decay of higher wave numbers.

Direct comparison of the stability results for large wave numbers with the stability conditions for plane evaporating surfaces is limited by the time dependence of the droplet radius $R(t)$, which causes changes in the droplet surface curvature, and by the fact that for large n the flow in the vapor phase will be approximately irrotational, as can be seen from Eq. (31)–(33). The latter is probably related to the observation of (Prosperetti and Plesset, 1984, p. 1601) that in the stable case, which for plane surfaces corresponds to large wave numbers, there is no vorticity in the vapor. Nevertheless, with certain limitations one can do the comparison and show that the stability condition is the same in both the cases. The details are provided in Appendix B.

It is interesting to compare our results for evaporating droplets and the results for expanding spherical flames (Istratov and Librovich, 1969) with those for spherical bubbles (Birkhoff, 1954, 1956; Plesset, 1954). In the latter case, there is no flow through the bubble surface and therefore the perturbed flow remains irrotational.

One sees from the comparison that the results are opposite. The growing bubble ($R \to \infty$) is stable and the collapsing bubble ($R \to 0$) is unstable. On the other hand, the expanding flame ($R \to \infty$) is unstable and evaporating droplets ($R \to 0$), as we have just shown, are stable.

3. Stability of a thin expanding spherical shell

3.1. Statement of the problem

Consider a thin spherical liquid shell of density ρ and surface tension σ expanding in a gas medium as shown in Fig. 3. The shell is characterized by its mean geometric radius $R(t)$ and its thickness $h(t)$. This model describes the late stage of explosive boiling.

The instability of an expanding liquid shell is stronger for boiling in a gas. This results from the large difference in density between liquid and gas, which facilitates the motions of shell segments. Therefore, we analyze this case.

We assume that:

1. The shell is thin relative to its radius ($h \ll R$);
2. The unperturbed (base) solution is spherically symmetric;
3. The liquid is inviscid and incompressible;
4. The flows in the outer gas and internal vapor bubble are negligible;
5. Evaporation from the outer surface of the droplet is negligible;
6. The pressure in the host gas p_∞ and the inner bubble p_i is constant and uniform.

Assumption 1 corresponds to later stages of explosive boiling. Assumptions 2 and 3 were discussed in Section 2.1. Assumption 4 follows the analysis of explosive boiling of Shusser and Weihs (1999). Assumption 5 is justified by the results of Section 2.

Assumption 6 corresponds to the existence of very weak evaporation into the inner bubble.

Because it is weak, one can neglect its influence on the shell mass and the stability, but due to the low density of the vapor it is sufficient to support constant pressure within the bubble.

We utilize the assumption of a thin shell by neglecting quantities of orderh^2/R^2 both in the base solution and in the perturbed flow.

3.2. Base solution

Let $4\pi M$ be the mass of the shell. Then from the conservation of mass

$$4\pi M = 4\pi h R^2 \rho \left(1 + \frac{h^2}{12R^2}\right) \tag{49}$$

and after neglecting the second-order quantities

$$hR^2 = \frac{M}{\rho} = \text{const} \tag{50}$$

To this approximation the flow-field in the shell is (the dot denotes a time derivative)

$$v = \frac{R^2}{r^2}\dot{R} \tag{51}$$

Then from the unsteady Bernoulli equation of hydrodynamics (Lamb, 1932) and the boundary conditions at both surfaces, one obtains in the linear approximation the equation for the shell radius

$$\ddot{R} + \frac{4\sigma}{M}R - \frac{(p_i - p_\infty)}{M}R^2 = 0 \tag{52}$$

This equation that remains valid even when p_i and p_∞ are time dependent, does not include a $\dot{R}$ term. This means that there is no damping term in the equation and therefore thin shell oscillations do not decay or amplify in the linear approximation.

Integrating Eq. (52), we obtain for the expanding shell

$$\dot{R} = \sqrt{\frac{2}{3}bR^3 - aR^2 + c} \tag{53}$$

where

$$a = \frac{4\sigma}{M}; \qquad b = \frac{p_i - p_\infty}{M} \tag{54}$$

and c is defined by initial conditions. For the contracting shell, one has to change the sign of the right-hand side of Eq. (53).

The expression within the radical in Eq. (53) must be positive. This can be considered as a condition on the shell radius R for sustaining a thin shell.

Eq. (53) can also be integrated to obtain an implicit expression for $R(t)$

$$t = \int_{R_0}^{R} \frac{\mathrm{d}R}{\sqrt{\frac{2}{3}bR^3 - aR^2 + c}} \tag{55}$$

Here $R_0 = R(0)$. The integral in Eq. (55) can be expressed as an elliptic function

$$R = e_3 + \frac{e_1 - e_3}{sn^2\left\{t\sqrt{\frac{b}{6}(e_1 - e_3)};\ \sqrt{\frac{e_2 - e_3}{e_1 - e_3}}\right\}} \tag{56}$$

where e_1, e_2, e_3 are the zeros of the equation

$$4z^3 - \frac{6a}{b}z^2 + \frac{6c}{b} = 0 \tag{57}$$

To illustrate the behavior of the solutions, we plotted them in Fig. 4 in terms of $x = bR/a$ as a function of $\tau = t\sqrt{a}$ for different values of $C = cb^2/a^3$. Both initially expanding and initially contracting shells are considered.

One sees that due to the shell becoming thinner while the pressure difference $p_i - p_\infty$ is constant, the shell expansion rate always increases. Such a behavior is prone to instabilities, which is indeed the case, as we shall see later.

It should be noted that for very large values of the shell radius R the assumption of the constant pressure inside the shell would no longer be valid. On the other hand, the influence of the pressure change on the shell stability will be limited, as we shall show later (see discussion after Eq. (81)).

3.3. Shell thickness perturbations

We perturb the base solution so that the shell radius and the shell thickness are now $R(t) + \eta(t;\ \theta;\ \varphi)$ and $h(t) + \xi(t;\ \theta\ \varphi)$. The perturbations are small and therefore $\eta \ll R$ and $\xi \ll h$ and the terms of order $O(\eta^2)$ and $O(\xi^2)$ are negligible.

The perturbed shell is situated between two slightly perturbed spheres. Their equations are

$$r = R \mp \frac{h}{2} + \eta \mp \frac{\xi}{2} \tag{58}$$

From conservation of mass

$$4\pi M = \rho(V_2 - V_1) \tag{59}$$

where V_1 and V_2 are the volumes of the inner and outer perturbed spheres, respectively. To linear approximation

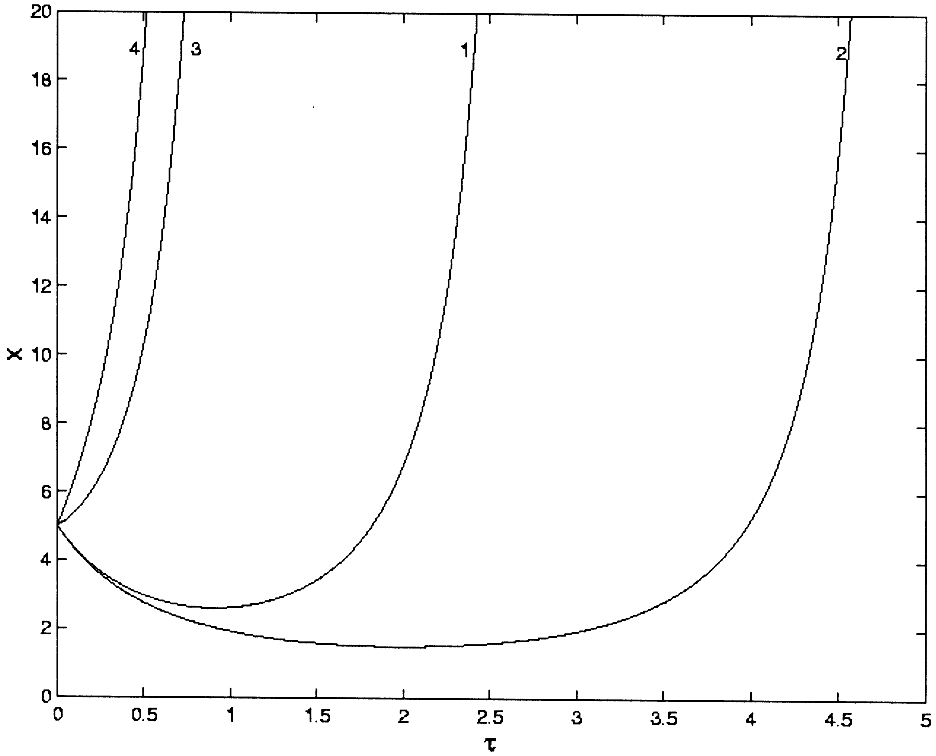

Fig. 4. Expansion of a thin liquid shell: 1 — initially contracting, $C = -5$; 2 — initially contracting, $C = 0$; 3 — initially expanding, $C = -50$; 3 — initially expanding, $C = 100$. $x = bR/a$, $\tau = t\sqrt{a}$, $C = cb^2/a^3$; a, b, c are defined in Eqs. (53) and (54).

$$V_1 = \frac{4}{3}\pi\left(R - \frac{h}{2}\right)^3 + \left(R - \frac{h}{2}\right)^2 \int_0^{2\pi}\int_0^{\pi}\left(\eta - \frac{\xi}{2}\right) d\theta d\varphi \tag{60}$$

$$V_2 = \frac{4}{3}\pi\left(R + \frac{h}{2}\right)^3 + \left(R + \frac{h}{2}\right)^2 \int_0^{2\pi}\int_0^{\pi}\left(\eta + \frac{\xi}{2}\right) \mathrm{d}\theta\, \mathrm{d}\varphi \tag{61}$$

Substituting Eqs. (50), (60) and (61) into Eq. (59) we obtain

$$\int_0^{2\pi}\int_0^{\pi}\left[\left(R^2 + \frac{h^2}{4}\right)\xi + 2Rh\eta\right] \mathrm{d}\theta\, \mathrm{d}\varphi = 0 \tag{62}$$

One can conclude that there exist two types of perturbations (see Fig. 3). Utilizing the assumption of a thin shell, we neglect the h^2 term in Eq. (62) though the decomposition into two types of perturbations remains valid for any h/R. If the perturbation of the radius η is not identically zero then

$$\xi = -\frac{2h}{R}\eta \tag{63}$$

The perturbations of the shell radius are analogous to the antisymmetric (sinuous) perturbations observed in plane liquid films (Squire, 1953) or annular liquid jets (Meyer and Weihs, 1987). For spherical flows, they also cause perturbations of the shell thickness, given by Eq. (63).

It is possible to perturb the thickness leaving the shell radius unchanged provided the shell volume does not change, i.e., if

$$\int_0^{2\pi}\int_0^{\pi} \xi \,\mathrm{d}\theta\,\mathrm{d}\varphi = 0 \tag{64}$$

This type of perturbation is analogous to the symmetric (varicose) perturbations for the plane film (Squire, 1953). Any perturbation can be represented as a linear combination of symmetric and antisymmetric ones. Therefore, each type of perturbation can be analyzed separately. We begin the analysis for the antisymmetric case.

3.4. Antisymmetric perturbations

The perturbation potential is a solution of the Laplace equation and therefore the full potential of the perturbed flow Φ is given by

$$\Phi = -\frac{R^2\dot{R}}{r} + \left(\frac{a_1(t)}{r^{n+1}} + a_2(t)r^n\right)Y_n^m(\theta;\varphi) \tag{65}$$

Assuming for the perturbation η a solution of the form

$$\eta = a_3(t)Y_n^m(\theta;\varphi) \tag{66}$$

we find the functions $a_1(t)$, $a_2(t)$, $a_3(t)$ from the boundary conditions, which are two kinematic boundary conditions (Lamb, 1932, p. 7)

$$v_r = \dot{R}\left(1-\frac{h}{R}\right) + \frac{\partial\eta}{\partial t}\left(1-\frac{h}{R}\right) + \frac{3h\dot{R}}{R^2}\eta, \quad r = R+\eta+\frac{h}{2}\left(1-\frac{2\eta}{R}\right) \tag{67}$$

$$v_r = \dot{R}\left(1+\frac{h}{R}\right) + \frac{\partial\eta}{\partial t}\left(1+\frac{h}{R}\right) - \frac{3h\dot{R}}{R^2}\eta, \quad r = R+\eta-\frac{h}{2}\left(1-\frac{2\eta}{R}\right) \tag{68}$$

and the conservation of momentum

$$\frac{p_\infty - p_i}{\rho} + \frac{\sigma}{\rho}(\Lambda_1 + \Lambda_2) = \left(\frac{\partial \Phi}{\partial t} + \frac{v_r^2}{2}\right)\Big|_{r=R+\eta-\frac{h}{2}\left(1-\frac{2\eta}{R}\right)} - \left(\frac{\partial \Phi}{\partial t} + \frac{v_r^2}{2}\right)\Big|_{r=R+\eta+\frac{h}{2}\left(1-\frac{2\eta}{R}\right)} \tag{69}$$

Here v_r is the radial component of the velocity and Λ_1, Λ_2 are curvatures of the inner and outer surfaces, respectively. The condition (69) has been obtained by combining the conservation equations for the normal component of momentum at the inner and outer interfaces, so the pressure in the liquid can be eliminated.

From Eqs. (67)–(69) the following system of equations is obtained

$$\frac{da_3}{dt} + \frac{2\dot{R}}{R}a_3 = \tilde{a}_2 - \tilde{a}_1 \tag{70}$$

$$\frac{(n+1)}{2}\tilde{a}_2 + \frac{n}{2}\tilde{a}_1 = 0 \tag{71}$$

$$R\frac{d}{dt}(\tilde{a}_1 - \tilde{a}_2) - 2\dot{R}(\tilde{a}_1 - \tilde{a}_2) + \frac{2a_3}{R}\left[2R\ddot{R} - 3\dot{R}^2 - \frac{\sigma}{\rho}\frac{(n-1)(n-2)}{h}\right] = 0 \tag{72}$$

Here

$$\tilde{a}_1 = \frac{(n+1)a_1(t)}{R^{n+2}}; \qquad \tilde{a}_2 = na_2(t)R^{n-1} \tag{73}$$

Eliminating $\tilde{a}_1$ and $\tilde{a}_2$ one obtains

$$\frac{d^2a_3}{dt^2} + \left(\frac{a(n-1)(n+2)}{2} - 2\ddot{R}\right)a_3 = 0 \tag{74}$$

where the constant a is defined in Eq. (54).

Taking the unperturbed radius R as an independent variable and using Eqs. (52)–(53), we retrieve

$$\left(\frac{2}{3}bR^3 - aR^2 + c\right)\frac{d^2a_3}{dR^2} + (bR^2 - aR)\frac{da_3}{dR} + \left(\frac{a\left(n^2+n+2\right)}{2} - 2bR\right)a_3 = 0 \tag{75}$$

We are interested in the behavior of the solution for $t \to \infty$, i.e. $R \to \infty$. Therefore we neglect the term of order R^{-2} assuming

$$\frac{2}{3}bR^3 - aR^2 + c \approx \frac{2}{3}bR^3 - aR^2 \tag{76}$$

Then after taking new variables

$$x = \frac{3a}{2bR}; \qquad y = \frac{a_3}{x^2} \tag{77}$$

the hypergeometric equation (Whittaker and Watson, 1927) is obtained

$$x(x-1)\frac{\mathrm{d}^2y}{\mathrm{d}x^2}+\left[(\alpha+\beta+1)x-\gamma\right]\frac{\mathrm{d}y}{\mathrm{d}x}+\alpha\beta y=0 \tag{78}$$

Here

$$\alpha=2+\sqrt{\frac{n^2+n+2}{2}};\quad \beta=2-\sqrt{\frac{n^2+n+2}{2}};\quad \gamma=\frac{9}{2} \tag{79}$$

Hence the amplitude of the shell radius perturbation a_3 is

$$\begin{aligned} a_3=\frac{1}{R^2}\Bigg[&C_1F\left(2+\sqrt{\frac{n^2+n+2}{2}};2-\sqrt{\frac{n^2+n+2}{2}};\frac{9}{2};\frac{3a}{2bR}\right)\\ &+C_2R^{7/2}F\left(-\frac{3}{2}+\sqrt{\frac{n^2+n+2}{2}};-\frac{3}{2}-\sqrt{\frac{n^2+n+2}{2}};-\frac{5}{2};\frac{3a}{2bR}\right)\Bigg] \end{aligned} \tag{80}$$

where F is the hypergeometric series (Whittaker and Watson, 1927).

Therefore when $R\to\infty$

$$\frac{a_3}{R}\sim\frac{C_1}{R^3}+C_2R^{1/2} \tag{81}$$

For stability a_3/R must remain bounded. Therefore, one of the solutions is always unstable and the conclusion is that the expansion of a thin liquid shell is unstable for antisymmetric perturbations. It can be noted that the instability is relatively weak, growing as $R^{1/2}$.

We now see that the influence of pressure variations inside the shell on the perturbations is limited because $3a/2bR$ is small for large R and hence $F\approx 1$.

As in the previous section, one can define characteristic times for the base flow τ_R and the perturbations τ_a as the leading order terms in $R/\dot{R}$ and $a_3/(\mathrm{d}a_3/\mathrm{d}t)$, i.e. $\tau_R=\sqrt{3/(2a)}$ and $\tau_a=2\tau_R/3$. One sees that these times are close and therefore despite fast increase of the shell radius the perturbations have enough time to grow and destabilize the process.

3.5. Second-order approximation of the base solution

Symmetric perturbations are perturbations of the shell thickness. The first-order approximation in h/R corresponds to a plane layer, rather than a shell. Therefore, in analyzing stability of symmetric perturbations we must retain the terms of order $\mathrm{O}(h^2/R^2)$ in the base solution.

Repeating the calculations of Section 3.2 including the $O(h^2/R^2)$ terms we obtain the shell thickness h and the flow potential Φ are now

$$h = \frac{M}{\rho R^2}\left(1 - \frac{M^2}{12\rho^2 R^6}\right) \tag{82}$$

$$\Phi = -\frac{R^2}{r}\dot{R}\left(1 - \frac{3h^2}{4R^2}\right) \tag{83}$$

Instead of Eq. (52) the equation for the shell radius is

$$\left(1 - \frac{M^2}{12\rho^2 R^6}\right)\ddot{R} + \frac{4\sigma}{M}R\left(1 + \frac{M^2}{4\rho^2 R^6}\right) - \frac{(p_i - p_\infty)}{M}R^2 = 0 \tag{84}$$

Integrating once

$$\dot{R} = \sqrt{2c\text{-}a\left[R^2 + F_1(R) - F_2(R)\right] + \frac{2}{3}b\left[R^3 + F_3(R)\right]} \tag{85}$$

where a, b, c are defined as in Section 3.2 and

$$F_1(R) \equiv \frac{2}{3}\sqrt[3]{\frac{m}{3}}\ln\frac{\left(R^2 - \sqrt[3]{\frac{m}{3}}\right)^2}{R^4 + R^2\sqrt[3]{\frac{m}{3}} + 3\sqrt{\frac{m^2}{9}}} \tag{86}$$

$$F_2(R) \equiv \frac{4}{3}\sqrt[6]{3}\sqrt[3]{m}\ \mathrm{arctg}\left(\frac{2R^2}{\sqrt[6]{3}\sqrt[3]{m}} + \frac{1}{\sqrt{3}}\right) \tag{87}$$

$$F_3(R) \equiv \frac{1}{2}\sqrt{\frac{m}{3}}\ln\frac{R^3 - \sqrt{\frac{m}{3}}}{R^3 + \sqrt{\frac{m}{3}}} \tag{88}$$

$$m = \frac{M^2}{4\rho^2} \tag{89}$$

The radius $R(t)$ can be calculated implicitly

$$t = \int_{R_0}^{R} \frac{\mathrm{d}R}{\sqrt{2c - a\left[R^2 + F_1(R) - F_2(R)\right] + \frac{2}{3}b\left[R^3 + F_3(R)\right]}} \tag{90}$$

To verify the influence of the second order correction on the base flow, we plotted the solution for both initially contracting (Fig. 5(a)) and initially expanding (Fig. 5(b)) shells. The calculations were made for $C = 0$ and different values of $\mu = mb^6/a^6$. First-order approximation corresponds to $\mu = 0$.

One sees from Fig. 5(a) that larger values of μ cause prolongation of the contracting phase but they are of lesser importance for the expanding phase. For the initially expanding shell (Fig. 5(b)), fast growth of x makes the second-order correction very small. We see from Fig. 5(b) that μ should be very large to have any influence on the solution. One can conclude that for thin expanding shells, which correspond to small values of μ, the second-order correction to the base solution is completely negligible though it is important for the analysis of perturbations, as we shall see later.

3.6. Symmetric perturbations

Proceeding as in Section 3.4 we look for a solution for the thickness perturbation ξ of the form

$$\xi = a_3(t) Y_n^m(\theta; \varphi) \tag{91}$$

with the potential in the perturbed flow

$$\Phi = -\frac{R^2}{r}\dot{R}\left(1 - \frac{3h^2}{4R^2}\right) + \left(\frac{a_1(t)}{r^{n+1}} + a_2(t)r^n\right)Y_n^m(\theta; \varphi) \tag{92}$$

Instead of Eqs. (67)–(69) the boundary conditions are now

$$v_r = \dot{R} + \frac{\dot{h} + \dot{\xi}}{2}, \qquad r = R + \frac{h + \xi}{2} \tag{93}$$

$$v_r = \dot{R} - \frac{\left(\dot{h} + \dot{\xi}\right)}{2}, \quad r = R - \frac{(h + \xi)}{2} \tag{94}$$

$$\frac{p_\infty - p_i}{\rho} + \frac{\sigma}{\rho}(\Lambda_1 + \Lambda_2) = \left(\frac{\partial \Phi}{\partial t} + \frac{v_{\mathrm{r}}^2}{2}\right)\Big|_{r=R-\frac{(h+\xi)}{2}} - \left(\frac{\partial \Phi}{\partial t} + \frac{v_{\mathrm{r}}^2}{2}\right)\Big|_{r=R+\frac{(h+\xi)}{2}} \tag{95}$$

and the equations for the amplitudes are

$$\frac{\mathrm{d}a_3}{\mathrm{d}t} + \frac{2\dot{R}}{R}\left(1 + \frac{3h^2}{4R^2}\right)a_3 = \frac{h}{2R}\left[(n+2)\tilde{a}_1 + (n-1)\tilde{a}_2\right] \tag{96}$$

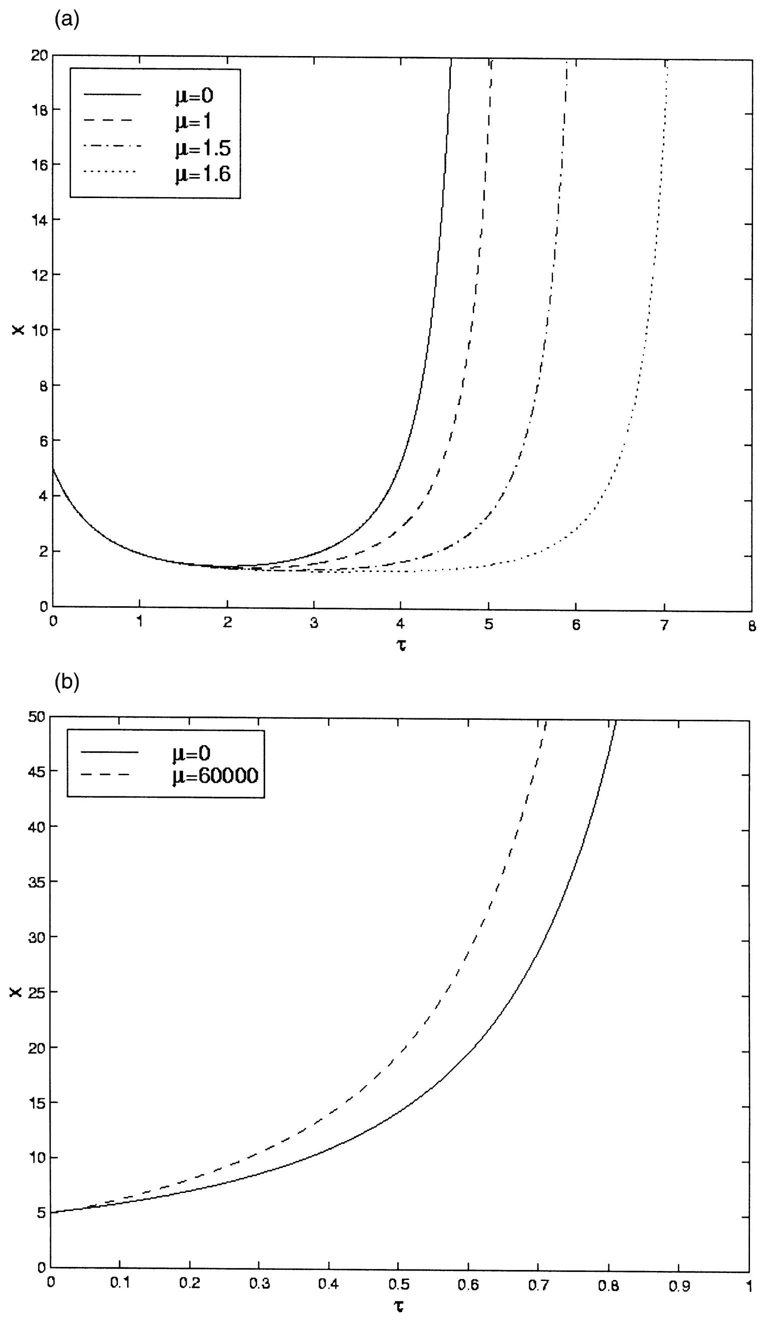

Fig. 5. Second-order approximation for expansion of a thin liquid shell: (a) initially contracting; (b) initially expanding. $x = bR/a$, $\tau = t\sqrt{a}$, $\mu = M^2b^6/(4\rho^2a^6)$; a, b are defined in Eq. (54).

$$\frac{3h\dot{R}}{R^2}a_3 = \left[1 + \frac{(n+2)(n+3)}{8}\frac{h^2}{R^2}\right]\tilde{a}_1 - \left[1 + \frac{(n-1)(n-2)}{8}\frac{h^2}{R^2}\right]\tilde{a}_2 \tag{97}$$

$$\left[\ddot{R} - \frac{\sigma}{\rho}\frac{(n-1)(n+2)h}{R^3}\right]a_3 = \frac{h}{2}\left[\frac{\mathrm{d}}{\mathrm{d}t}(\tilde{a}_1 - \tilde{a}_2) - \frac{2\dot{R}}{R}(\tilde{a}_1 - \tilde{a}_2)\right] \tag{98}$$

where $\tilde{a}_1$, $\tilde{a}_2$ are still defined by Eq. (73).

We see from Eqs. (96)–(98) that the second-order terms in the base flow are significant. Neglecting the second-order terms and substituting Eq. (97) in Eq. (98), we obtain that the thickness perturbation a_3 vanishes identically.

Taking R as an independent variable and eliminating $\tilde{a}_1$, $\tilde{a}_2$ we obtain

$$\frac{\mathrm{d}^2a_3}{\mathrm{d}R^2} + P(R)\frac{\mathrm{d}a_3}{\mathrm{d}R} + Q(R)a_3 = 0 \tag{99}$$

where

$$P(R) = \frac{\ddot{R}}{\dot{R}^2} - \frac{6}{R} \tag{100}$$

$$Q(R) = \frac{\ddot{R}}{\dot{R}^2}\left(\frac{2R}{h^2} - \frac{1}{R}\right) + \frac{6}{R^2} - \frac{2\sigma}{\rho}\frac{(n-1)(n+2)}{\dot{R}^2R^2h} \tag{101}$$

From the leading terms of $P(R)$, $Q(R)$ for R sufficiently large

$$Q > 0; \qquad \frac{\mathrm{d}Q}{\mathrm{d}R} + 2PQ < 0 \tag{102}$$

and therefore (Birkhoff, 1956) each solution of Eq. (99) tends to infinity when $R \to \infty$.

To find the behavior of the solution for $R \to \infty$, we substitute in Eq. (99) the first terms in the asymptotic expansions of P and Q for large R

$$\frac{\mathrm{d}^2a_3}{\mathrm{d}R^2} - \frac{9}{2R}\frac{\mathrm{d}a_3}{\mathrm{d}R} + \frac{3R^4}{4m}a_3 = 0 \tag{103}$$

After taking

$$x = \frac{R^3}{\sqrt{12m}}; \qquad y = \frac{a_3}{R^{11/4}} \tag{104}$$

a Bessel equation is retrieved

$$\frac{\mathrm{d}^2y}{\mathrm{d}x^2} + \frac{1}{x}\frac{\mathrm{d}y}{\mathrm{d}x} + \left(1 - \frac{121}{144x^2}\right)y = 0 \tag{105}$$

Hence the general solution of Eq. (103) is

$$a_3 = R^{11/4}\left[C_1 J_{11/12}\left(\frac{R^3}{\sqrt{12m}}\right) + C_2 Y_{11/12}\left(\frac{R^3}{\sqrt{12m}}\right)\right] \tag{106}$$

Comparing the behavior of the shell thickness h and the amplitude of its perturbation a_3 one sees that when $R \to \infty$ and $h \to 0$

$$\frac{a_3}{h} \sim h^{-13/8} \xrightarrow[h\to 0]{} \infty \tag{107}$$

That is, there is strong instability for all wave numbers.

The characteristic time of the base flow τ_R remains the same in the second-order approximation due to negligible influence of the second-order correction on the base flow. For the perturbations, the characteristic time defined as previously now equals $0.8\tau_R$. We see that characteristic times for both types of perturbations are close.

3.7. Discussion

We obtained that both perturbations of the shell radius (antisymmetric) and perturbations of the shell thickness (symmetric) are unstable. When the shell radius R tends to infinity and the shell thickness h tends to zero, the appropriate perturbations normalized by R or h, respectively, are asymptotic to $\sqrt{R}$ and $h^{-13/8}$.

Squire (1953) has shown that for thin film stability both types of perturbations are unstable. In variance with our solution, however, in the plane case antisymmetric perturbations grow much faster than symmetric ones. For a spherical shell, we obtained weak instability for perturbations of the shell radius and strong instability for those of the thickness. The reason for this discrepancy lies in different velocity direction in the two cases. In Squire's problem the velocity was along the film (Kelvin–Helmholtz instability), while in our case the liquid shell accelerates normal to itself (Rayleigh–Taylor instability) (Drazin and Reid, 1981, pp. 14–22).

The fact that both shell radius and shell thickness are time-dependent in our spherical case does not change the general conclusion about stability but changes its nature because the most dangerous perturbations are now of a different type. The weak instability obtained for the antisymmetric perturbations may tie in with the related process of gas bubble growth with a constant pressure inside the bubble, which is stable (Birkhoff, 1954, 1956; Plesset, 1954; Plesset and Mitchell, 1956).

Growing instabilities of an expanding spherical shell will finally cause its rupture and fragmentation, as has been observed experimentally for explosive boiling (Hill and Sturtevant, 1990) and explosive exsolution within liquids (Mader et al., 1994; Mader et al., 1997). The mechanism for fragmentation, though not fully understood, is thought to be wall thinning due to hydrodynamic instabilities (Mader et al., 1996, p. 5558). Hence, one can expect the symmetric perturbations to lead to fragmentation sooner than the axisymmetric ones.

The goal of this section was to identify the most unstable perturbations for stability of explosive boiling. These are the symmetric (varicose) perturbations.

4. Stability of explosive boiling

4.1. Physical situation

The physical situation is depicted in Fig. 6. A vapor bubble of radius $R_1(t)$ grows within a highly superheated liquid droplet of radius $R_2(t)$, which is situated in liquid or gas medium. For simplicity, we assume that the bubble is situated in the center of the droplet. Though an approximation, this assumption was shown to be reasonable for a broad range of physical situations (Shusser and Weihs, 1999).

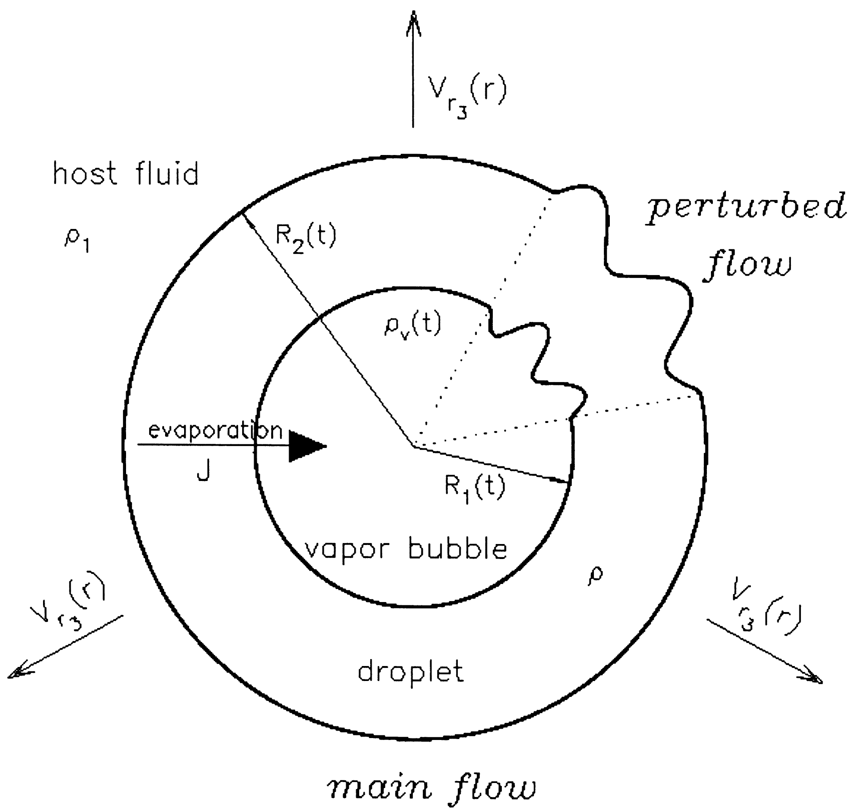

Fig. 6. Explosive boiling of a liquid droplet.

As in Section 2.1 we assume that all the fluids are inviscid and incompressible and the evaporation rate is constant and is not influenced by the perturbations. We also neglect the flow inside the vapor bubble (see Section 3.1). Utilizing the results of the previous sections we neglect the effects of possible evaporation from the outer surface of the droplet (Section 2) and consider only symmetric perturbations (Section 3).

An analysis equivalent to that in Section 2 shows that constant rate of evaporation results in constant rate of growth of the bubble radius (Shepherd and Sturtevant, 1982). Denoting this constant rate U, we write

$$R_1 = Ut \tag{108}$$

and using conservation of mass

$$\frac{R_2}{R_0} = \left[1 + (1-\alpha)\left(\frac{Ut}{R_0}\right)^3\right]^{1/3} \tag{109}$$

Here R_0 is the initial radius of the droplet; $\alpha = \rho_v/\rho$; ρ, ρ_v are the densities of the droplet liquid and the vapor, respectively.

Under these conditions the flow-field in the main flow is

$$V_{r_1} = 0 \tag{110}$$

$$V_{r_2} = V_{r_3} = \frac{(1-\alpha)U^3t^2}{r^2} \tag{111}$$

where the indices 1, 2, 3 correspond to the vapor bubble, the liquid droplet and the host fluid, respectively.

Using the Bernoulli equation one can calculate the pressure field

$$P_1 = G(t) + \frac{(1-\alpha)(3-\alpha)\rho U^2}{2} + \frac{2\sigma}{R_1} \tag{112}$$

$$P_2 = G(t) + \frac{2(1-\alpha)\rho U^3 t}{r}\left[1 - \frac{(1-\alpha)}{4}\frac{U^3t^3}{r^3}\right] \tag{113}$$

$$P_3 = p_\infty + \frac{2(1-\alpha)\rho_1 U^3 t}{r}\left[1 - \frac{(1-\alpha)}{4}\frac{U^3t^3}{r^3}\right] \tag{114}$$

Here p_∞ is the pressure far from the droplet; ρ_1 is the density of the host fluid; σ is the surface tension of the droplet liquid and $G(t)$ is a function of time.

4.2. Perturbations and boundary conditions

We add small symmetric perturbations $\varepsilon(\theta;\ \varphi;\ t)$ ($\varepsilon \ll R_1,\ R_2$) to both interfaces so their equations are now

$$r_1 = R_1(t) + \varepsilon(\theta;\ \varphi;\ t) \tag{115}$$

$$r_2 = R_2(t) - \varepsilon(\theta;\ \varphi;\ t) \tag{116}$$

From conservation of mass

$$\int_0^{2\pi}\int_0^{\pi} \varepsilon(\theta;\ \varphi;\ t)\sin\theta\,\mathrm{d}\theta\,\mathrm{d}\varphi = 0 \tag{117}$$

Distortion of the droplet shape causes perturbations of the velocity v'_{r_i}, v'_{θ_i}, v'_{φ_i} and the pressure p'_i ($i = 1, 2, 3$ for the vapor bubble, the liquid droplet and the host fluid, respectively). These perturbations satisfy the boundary conditions at the surface of the bubble and the surface of the droplet.

We write the conditions of conservation of mass, conservation of the tangential components of momentum and constancy of the evaporation rate at the surface of the unperturbed bubble $r = R_1$ as

$$v'_{r_1} = \frac{\partial\varepsilon}{\partial t} \tag{118}$$

$$v'_{r_2} + \varepsilon\frac{\partial V_{r_2}}{\partial r} = \frac{\partial\varepsilon}{\partial t} \tag{119}$$

$$v'_{\theta_1} = v'_{\theta_2} + \frac{1}{R_1}\frac{\partial\varepsilon}{\partial\theta}V_{r_2} \tag{120}$$

$$v'_{\varphi_1} = v'_{\varphi_2} + \frac{1}{R_1\sin\theta}\frac{\partial\varepsilon}{\partial\varphi}V_{r_2} \tag{121}$$

The kinematic conditions at the surface of the unperturbed droplet $r = R_2$ are

$$v'_{r_2} + \frac{\partial\varepsilon}{\partial t} = \varepsilon\frac{\partial V_{r_2}}{\partial r} \tag{122}$$

$$v'_{r_3} + \frac{\partial\varepsilon}{\partial t} = \varepsilon\frac{\partial V_{r_3}}{\partial r} \tag{123}$$

As in Section 3, conservation of the normal component of momentum at $r = R_1$ and at $r = R_2$

results in the dynamic boundary condition

$$\left(p_3' - \varepsilon\frac{\partial P_3}{\partial r}\right)|_{r=R_2} - p_1'|_{r=R_1} + \sigma\left(\Lambda_1 + \Lambda_2 - \frac{2}{R_1} - \frac{2}{R_2}\right)$$
$$= \left(p_2' - \varepsilon\frac{\partial P_2}{\partial r}\right)|_{r=R_2} - \left(p_2' + \varepsilon\frac{\partial P_2}{\partial r}\right)|_{r=R_1} \tag{124}$$

4.3. Perturbed flow

Recalling that the perturbed flow in the liquid droplet and in the host fluid is irrotational, and choosing appropriate solutions of the Laplace equation for the perturbation potential, we obtain

$$v_{r_3}' = -\frac{(n+1)f_3}{r^{n+2}}Y_n^m \tag{125}$$

$$v_{\theta_3}' = \frac{f_3}{r^{n+2}}\frac{\partial Y_n^m}{\partial\theta} \tag{126}$$

$$v_{\varphi_3}' = \frac{f_3}{r^{n+2}}\frac{1}{\sin\theta}\frac{\partial Y_n^m}{\partial\varphi} \tag{127}$$

$$p_3' = -\frac{\rho_1}{r^{n+1}}\left[\dot{f}_3 - \frac{(n+1)(1-\alpha)R_1^2\dot{R}_1f_3}{r^3}\right]Y_n^m \tag{128}$$

$$v_{r_2}' = \left(nf_2r^{n-1} - \frac{(n+1)g_2}{r^{n+2}}\right)Y_n^m \tag{129}$$

$$v_{\theta_2}' = \left(f_2\ r^{n-1} + \frac{g_2}{r^{n+2}}\right)\frac{\partial Y_n^m}{\partial\theta} \tag{130}$$

$$v_{\varphi_2}' = \left(f_2r^{n-1} + \frac{g_2}{r^{n+2}}\right)\frac{1}{\sin\theta}\frac{\partial Y_n^m}{\partial\varphi} \tag{131}$$

$$p_2' = -\rho\left[\dot{f}_2r^n + \frac{\dot{g}_2}{r^{n+1}} + \left(nf_2r^{n-1} - \frac{(n+1)g_2}{r^{n+2}}\right)\frac{(1-\alpha)R_1^2\dot{R}_1}{r^2}\right]Y_n^m + \Pi(t) \tag{132}$$

where $\Pi(t)$ is a function of time.

The perturbed flow within the vapor bubble will be rotational, because vorticity is created when the fluid flows through the distorted bubble surface (Section 2.4). Again following Landau (1944) and Istratov and Librovich (1969) and using the assumption of the absence of flow within the bubble in the base solution, one can write the pressure perturbation as a solution of the Laplace equation, of the form

$$p_1' = f(t) r^n Y_n^m \tag{133}$$

Integrating the linearized Euler equation, we obtain

$$v_{r_1}' = \left(-\frac{n f_1(t) r^{n-1}}{\rho_\mathrm{v}} + g_1(r) \right) Y_n^m \tag{134}$$

$$v_{\theta_1}' = \left(-\frac{f_1(t) r^{n-1}}{\rho_\mathrm{v}} + \hat{G}_2(r) \right) \frac{\partial Y_n^m}{\partial \theta} \tag{135}$$

$$v_{\varphi_1}' = \left(-\frac{f_1(t) r^{n-1}}{\rho_\mathrm{v}} + \hat{G}_3(r) \right) \frac{1}{\sin\theta} \frac{\partial Y_n^m}{\partial \varphi} \tag{136}$$

Substituting (134)–(136) into the continuity equation one obtains

$$\hat{G}_2 = \frac{1}{n(n+1)} \left(r \frac{\mathrm{d}g_1}{\mathrm{d}r} + 2 g_1 \right) \tag{137}$$

$$\hat{G}_3 = \hat{G}_2 \tag{138}$$

That is, the perturbed flow-field inside the vapor bubble depends on two unknown functions $f_1(t)$ and $g_1(r)$.

Finally, we write the perturbation ε as, using Eq. (117)

$$\varepsilon(\theta;\ \varphi;\ t) = f_4(t) Y_n^m(\theta;\ \varphi) \quad (n \neq 0) \tag{139}$$

4.4. The perturbation equations

By substituting Eqs. (125)–(136) into the boundary conditions Eqs. (118)–(124) the following equations are obtained

$$\frac{\mathrm{d}f_4}{\mathrm{d}t} = \tilde{g}_1 - \tilde{f}_1 \tag{140}$$

$$\frac{\mathrm{d}f_4}{\mathrm{d}t} + \frac{2(1-\alpha)\dot{R}_1}{R_1} f_4 = n\tilde{f}_2 - (n+1)\tilde{g}_2 \tag{141}$$

$$\frac{R_1}{\dot{R}_1}\frac{d\tilde{g}_1}{dt} + 2\tilde{g}_1 = n(n+1)\left(\tilde{f}_2 + \tilde{g}_2 + \frac{(1-\alpha)\dot{R}_1}{R_1}f_4\right) + (n+1)\tilde{f}_1 \tag{142}$$

$$\frac{df_4}{dt} + \frac{2(1-\alpha)\dot{R}_1 R_1^2}{R_2^3}f_4 = -\frac{nR_2^{n-1}}{R_1^{n-1}}\tilde{f}_2 + \frac{(n+1)R_1^{n+2}}{R_2^{n+2}}\tilde{g}_2 \tag{143}$$

$$\frac{df_4}{dt} + \frac{2(1-\alpha)\dot{R}_1 R_1^2}{R_2^3}f_4 = \tilde{f}_3 \tag{144}$$

$$\begin{aligned}
&\frac{d\tilde{f}_2}{dt}R_1\left(1 - \frac{R_2^n}{R_1^n}\right) + \tilde{f}_2\dot{R}_1\left[-(n-1)\left(1 - \frac{R_2^n}{R_1^n}\right) + n(1-\alpha)\left(1 - \frac{R_2^{n-3}}{R_1^{n-3}}\right)\right] \\
&+ \frac{d\tilde{g}_2}{dt}R_1\left(1 - \frac{R_1^{n+1}}{R_2^{n+1}}\right) + \tilde{g}_2\dot{R}_1\left[(n+2)\left(1 - \frac{R_1^{n+1}}{R_2^{n+1}}\right) - (n+1)(1-\alpha)\left(1 - \frac{R_1^{n+4}}{R_2^{n+4}}\right)\right] \\
&+ f_4\left\{\frac{(1-\alpha)}{R_1}\left[\left(R_1\ddot{R}_1 + 2\dot{R}_1^2\right)\left(1 + \frac{(1-\beta)R_1^2}{R_2^2}\right) - 2(1-\alpha)\dot{R}_1^2\left(1 + \frac{(1-\beta)R_1^5}{R_2^5}\right)\right]\right. \\
&\left. - \left[n(n+1) - 2\right]\frac{\sigma}{\rho}\left(\frac{1}{R_1^2} - \frac{1}{R_2^2}\right)\right\} + \frac{\beta}{n+1}\left(\frac{d\tilde{f}_3}{dt}R_2 + \frac{(1-\alpha)\dot{R}_1 R_1^2}{R_2^2}\tilde{f}_3\right) \\
&+ \frac{\alpha}{n}\left(\frac{d\tilde{f}_1}{dt}R_1 - (n-1)\dot{R}_1\tilde{f}_1\right) = 0
\end{aligned} \tag{145}$$

Here $\beta = \rho_1/\rho$ and

$$\tilde{f}_1 = \frac{nf_1 R_1^{n-1}}{\rho_v}; \quad \tilde{g}_1 = g_1[R(t)]; \quad \tilde{f}_2 = f_2 R_1^{n-1}; \quad \tilde{g}_2 = \frac{g_2}{R_1^{n+2}}; \quad \tilde{f}_3 = \frac{(n+1)f_3}{R_2^{n+2}} \tag{146}$$

Eliminating the other functions, we obtain the equation for the amplitude of the shape perturbation f_4

$$A(t)\frac{d^2 f_4}{dt^2} + B(t)\frac{df_4}{dt} + C(t)f_4 = 0 \tag{147}$$

The functions $A(t)$, $B(t)$, $C(t)$ are written out in Appendix C.

4.5. Stability analysis

We start by defining the conditions for stability. The process of explosive boiling occurs during a finite time until the droplet evaporates completely, i.e., until

$$t = t_{\mathrm{f}} = \frac{R_0}{U\alpha^{1/3}} \tag{148}$$

We propose to analyze the stability by investigating the behavior of the solution of Eq. (147) when $t \to t_{\mathrm{f}}$. Our method is based on the assumption that for $0 < t < t_{\mathrm{f}}$ the perturbation remains sufficiently small for the linear approximation to be possible. Therefore, it can prove only instability of the process. On the other hand, the physical situation at the limit $t \to t_{\mathrm{f}}$ closely resembles the base flow of Section 3 and therefore instability is probable.

Taking a new variable

$$\tau = t_{\mathrm{f}} - t \tag{149}$$

we see that

$$R_1 = \frac{R_0}{\alpha^{1/3}}\left(1 - \frac{U\alpha^{1/3}}{R_0}\tau\right) \tag{150}$$

We are interested in the limit $\tau \to 0$, so one can neglect the second-order terms in τ

$$R_2 = \frac{R_0}{\alpha^{1/3}} - (1-\alpha)U\tau \tag{151}$$

One sees that in the linear approximation

$$R_2 - R_1 = \alpha U \tau \tag{152}$$

and hence concludes that for stability the shape perturbation ε must tend to zero at least as $\mathrm{O}(\tau)$.

From Appendix C

$$A(t) = \left(\frac{\beta}{n+1} - \frac{\alpha}{n}\right)\frac{R_0}{\alpha^{1/3}} + U\tau\left(\frac{\alpha}{n} - \frac{(1-\alpha)\beta}{n+1}\right) + \mathrm{O}(\tau^2) \tag{153}$$

$$B(t) = -\frac{2R_0}{n\alpha^{1/3}\tau} + U\left[\frac{2-(n+4)\alpha}{n} - \frac{3(1-\alpha)\beta}{n+1}\right] + \mathrm{O}(\tau) \tag{154}$$

$$C(t) = -\frac{4(1-\alpha)U}{n\tau} + \frac{(1-\alpha)\alpha^{4/3}U^2}{R_0}\left[n+2-\frac{2}{n(2n+1)} - \frac{2(n-1)\beta}{n+1}\right] + \mathrm{O}(\tau) \tag{155}$$

and taking new variables

$$x = \frac{U\alpha^{1/3}}{R_0}\tau; \qquad y = \frac{\alpha^{1/3}}{R_0}f_4 \tag{156}$$

one can write the approximate form of Eq. (147) as

$$x(a_1x + a_2)\frac{d^2y}{dx^2} + (b_1x + b_2)\frac{dy}{dx} + (c_1x + c_2)y = 0 \tag{157}$$

where

$$a_1 = \frac{\alpha}{n} - \frac{\beta}{n+1} + \frac{\alpha\beta}{n+1}; \qquad a_2 = \frac{\beta}{n+1} - \frac{\alpha}{n} \tag{158}$$

$$b_1 = \frac{2-(n+4)\alpha}{n} - \frac{3(1-\alpha)\beta}{n+1}; \qquad b_2 = -\frac{2}{n} \tag{159}$$

$$c_1 = \alpha(1-\alpha)\left(n + 2 - \frac{2}{n(2n+1)} - \frac{2(n-1)\beta}{n+1}\right); \qquad c_2 = -\frac{4(1-\alpha)}{n} \tag{160}$$

where $n \neq 0$ due to conservation of mass.

Before analyzing the solutions of Eq. (157) it should be noted that the coefficients Eqs. (158)–(160) depend on the density ratios α and β. It is clear that small changes in α or β can change the solution behavior only slightly. Hence, one can exclude certain specific values of these quantities, which would cause difficulties in the analysis. We thus assume that $a_2 \neq 0$ and that b_2/a_2 is not equal to any positive or negative integer.

No general analytic solutions for Eq. (157) are known. Therefore, we study the behavior of the solution when $x \to 0$ using the method of Fröbenius (Kamke, 1944). Substituting in Eq. (157)

$$y = x^p\left(1 + \sum_{k=1}^{\infty} q_k x^k\right) \tag{161}$$

one obtains two possible solutions

$$p = 0 \tag{162}$$

$$q_1 = -\frac{c_2}{b_2} \tag{163}$$

$$q_{k+1} = -\frac{\left(q_{k-1}c_1 + q_k\left\{k\left[a_1(k-1) + b_1\right] + c_2\right\}\right)}{(k+1)(ka_2 + b_2)}, \quad k = 1, 2, 3, \ldots \tag{164}$$

and

$$p = 1 - \frac{b_2}{a_2} \tag{165}$$

$$q_1 = \frac{(b_1 a_2 - b_2 a_1)(a_2 - b_2) + c_2 a_2^2}{a_2^2(b_2 - 2a_2)} \tag{166}$$

$$q_{k+1} = \frac{q_{k-1} c_1 a_2^2 + q_k \left\{ \left[(k+1)a_2 - b_2\right]\left[b_1 a_2 + a_1(k a_2 - b_2)\right] + c_2 a_2^2 \right\}}{(k+1)\left[b_2 - (k+2)a_2\right]a_2^2}, \tag{167}$$

$k = 1, 2, 3, \ldots$

The assumptions we made guarantee the solutions' existence for each k. Therefore when $k \to 0$

$$y_1 \sim x^{1-\frac{b_2}{a_2}} \tag{168}$$

$$y_2 = \mathrm{O}(1) \tag{169}$$

Returning to physical variables, we can write for these solutions

$$\frac{\varepsilon}{R_2 - R_1} \sim (t_\mathrm{f} - t)^{\frac{2(n+1)}{\beta n - \alpha(n+1)}} \tag{170}$$

$$\frac{\varepsilon}{R_2 - R_1} \sim \frac{1}{(t_\mathrm{f} - t)} \tag{171}$$

Thus, there exist two solutions Eqs. (170) and (171) for symmetric perturbations of the process of explosive boiling of a liquid droplet. The stability of the former depends on the ratio of the densities of the vapor and the host fluid α/β. For low density of the host fluid ($\alpha > \beta$) the solution Eq. (170) is also unstable and grows faster than Eq. (171). When $\beta > \alpha$ only low wave numbers are unstable in Eq. (170). For high density of the host liquid, the solution Eq. (170) is stable. That means that the droplet breakup is easier in the gas medium than in the liquid, which is a physically reasonable result.

On the other hand, the solution Eq. (171) is always unstable. One can therefore conclude that the process of the explosive boiling of a liquid droplet is unstable.

5. Conclusions

Two related problems dealing with the stability of explosive boiling of a liquid droplet were considered. Evaporation of a highly superheated droplet is shown to be stable and we studied the stability of a thin expanding liquid shell. The results of the former problem can be also applied to contracting spherical flames while investigation of the latter may throw some light on the process of droplet breakup at the final stages of the boiling.

The results of these related problems were used to justify the assumptions necessary in studying the general case of explosive boiling stability. It was found that the process is unstable as observed in the experiments of Shepherd and Sturtevant (1982). The instability was obtained for all wave numbers which again is consistent with the observation of (Shepherd and Sturtevant, 1982, p. 388) that the roughening of the bubble surface occurs on many length scales.

Finally, it should be mentioned that though the theory has been developed for the problem of explosive boiling, the results of Sections 3 and 4 may be more generally applicable to situations in which gaseous bubbles grow internally within liquid shells (e.g., due to chemical reactions or exsolution of gases from a liquid).

Acknowledgements

This paper is based on parts of M. Shusser's Doctoral thesis. The study was supported by the Fund for Promotion of Research at Technion.We would like to thank Prof. A. Prosperetti, Associate Editor of the International Journal of Multiphase Flow, for his help in improving the presentation of this work. We also thank the referees for valuable comments.

Appendix A. Estimation of the drop surface temperature perturbations

The goal of this appendix is to justify the assumption of absence of the influence of droplet surface temperature perturbations on the evaporation rate of a highly superheated liquid droplet made in Section 2.1. We shall now calculate the droplet surface temperature and its perturbation and show that the latter can be neglected.

We start by calculating the droplet surface temperature itself. By calculating the change, we can show that the assumption of constant surface temperature was indeed reasonable.

Due to absence of the flow within the droplet in the unperturbed solution, the temperature field inside the droplet $T(r, t)$ is governed by the following equation and initial and boundary conditions:

$$\frac{\partial T}{\partial t} = \frac{D}{r^2}\frac{\partial}{\partial r}\left(r^2\frac{\partial T}{\partial r}\right), \tag{A.1}$$

$$t = 0 \quad T = T_0, \tag{A.2}$$

$$r = 0 \quad T \text{ is finite}, \tag{A.3}$$

$$r = R(t) \quad \frac{\partial T}{\partial r} = -\frac{LJ}{k}. \tag{A.4}$$

Here D is the thermal diffusivity, L is the latent heat of evaporation, k is the heat conductivity and T_0 is the initial temperature of the droplet, which is close to the superheat limit.

Taking a new variable

$$y = \frac{R^2}{r} - R, \tag{A.5}$$

one obtains

$$\frac{\partial T}{\partial t} + \left(\frac{2R}{r} - 1\right)\dot{R}\frac{\partial T}{\partial y} = D\frac{R^4}{r^4}\frac{\partial^2 T}{\partial y^2}, \tag{A.6}$$

$$t = 0 \quad T = T_0, \tag{A.7}$$

$$y = 0 \quad \frac{\partial T}{\partial y} = \frac{LJ}{k}, \tag{A.8}$$

$$y \to \infty \quad T \text{ is finite.} \tag{A.9}$$

Following Plesset and Zwick (1952), we assume that the temperature variations are appreciable only in a thin thermal boundary layer adjacent to the droplet surface. Then in the zero-order approximation ($r \approx R$)

$$\frac{\partial T}{\partial t} + \dot{R}\frac{\partial T}{\partial y} = D\frac{\partial^2 T}{\partial y^2}. \tag{A.10}$$

Defining

$$\Theta = T - T_0, \tag{A.11}$$

and using

$$\dot{R} = -\frac{J}{\rho}, \tag{A.12}$$

we obtain

$$\frac{\partial \Theta}{\partial t} - \frac{J}{\rho}\frac{\partial \Theta}{\partial y} = D\frac{\partial^2 \Theta}{\partial y^2}, \tag{A.13}$$

$$t = 0 \quad \Theta = 0, \tag{A.14}$$

$$y = 0 \quad \frac{\partial \Theta}{\partial y} = \frac{LJ}{k}, \tag{A.15}$$

$$y \to \infty \quad \Theta \text{ is finite.} \tag{A.16}$$

Eq. (A.13) with the conditions Eqs. (A.14)–(A.16) can be solved by using Laplace transformation. We define

$$v = \int_0^\infty \mathrm{e}^{-st} \Theta \, \mathrm{d}t. \tag{A.17}$$

Substituting in Eqs. (A.13)–(A.16), one obtains

$$\frac{\mathrm{d}^2 v}{\mathrm{d}y^2} + \frac{J}{\rho D} \frac{\mathrm{d}v}{\mathrm{d}y} - \frac{sv}{D} = 0, \tag{A.18}$$

$$y = 0 \quad \frac{\mathrm{d}v}{\mathrm{d}y} = \frac{LJ}{ks}, \tag{A.19}$$

$$y \to \infty \quad v \text{ is finite.} \tag{A.20}$$

The solution of Eq. (A.18)–(A.20) is

$$v = -\frac{LJ}{ks} \frac{\mathrm{e}^{-\frac{J}{2\rho D} y} \mathrm{e}^{-y\sqrt{\frac{J^2}{4\rho^2 D^2} + \frac{s}{D}}}}{\left(\frac{J}{2\rho D} + \sqrt{\frac{J^2}{4\rho^2 D^2} + \frac{s}{D}} \right)}. \tag{A.21}$$

Writing the right-hand side of Eq. (A.21) as a sum of partial fractions and using the tables and properties of Laplace transformation (Carslow and Jaeger, 1959, pp. 298–301, 494–496), one can show that Eq. (A.21) corresponds to the following solution for the unsteady temperature field inside the droplet

$$T = T_0 + \frac{LJ}{k}\left[\frac{1}{2}\left(y + \frac{J}{\rho}t + \frac{\rho D}{J}\right)\mathrm{erfc}\left(\frac{y + \frac{J}{\rho}t}{2\sqrt{Dt}}\right) - \frac{\rho D}{2J}\mathrm{e}^{-\frac{J}{\rho D}y}\mathrm{erfc}\left(\frac{y - \frac{J}{\rho}t}{2\sqrt{Dt}}\right) - \sqrt{\frac{Dt}{\pi}}\mathrm{e}^{-\frac{\left(y + \frac{J}{\rho}t\right)^2}{4Dt}}\right]. \tag{A.22}$$

Then the surface temperature T_s is

$$T_{\mathrm{s}} = T_0 - \frac{L}{c} + \frac{LJ}{k}\left[\left(\frac{J}{2\rho}t + \frac{\rho D}{J}\right)\mathrm{erfc}\left(\frac{J}{2\rho}\sqrt{\frac{t}{D}}\right) - \sqrt{\frac{Dt}{\pi}}\mathrm{e}^{-\frac{J^2 t}{4\rho^2 D}}\right]. \tag{A.23}$$

Here c is the specific heat of the droplet liquid.

As time increases, the expression in the square brackets in (A.23) tends to zero very fast. For example, for a butane droplet (see Shepherd and Sturtevant, 1982; Shusser, 1997; Shusser and Weihs, 1999 for the relevant properties of superheated butane) the characteristic time for the surface temperature change $4\rho^2 D/J^2$ is about 2.6 μs, while the evaporation of a droplet with a diameter of 1 mm will take about 1390 μs. Therefore, with a good accuracy one can approximate the surface temperature by its value for $t \to \infty$.

$$T_{\mathrm{s}} = T_0 - \frac{L}{c}. \tag{A.24}$$

For a butane droplet, the superheat limit $T_0 = 378$ K, the specific heat $c = 2390$ J/(kg K) and the heat of evaporation (corrected for the use of the heat of superheating in the evaporation) $L = 1.34 \times 10^5$ J/kg. Then $T_{\mathrm{s}} = 322$ K. The boiling temperature of butane at the atmospheric pressure is 272.7 K. One sees that the droplet remains highly superheated during the evaporation and therefore the influence of surface temperature change on the evaporation is limited.

Indeed, in the linear approximation the evaporation rate change ΔJ will be

$$\Delta J = -\frac{\partial J}{\partial T}\frac{L}{c}. \tag{A.25}$$

If one uses the Hertz–Knudsen equation for the evaporation rate (Prosperetti and Plesset, 1984, pp. 1591–1592), then in a reasonable approximation

$$\frac{\partial J}{\partial T} = \frac{J}{2T_0}. \tag{A.26}$$

Therefore

$$\frac{\Delta J}{J} = -\frac{L}{2T_0 c}. \tag{A.27}$$

Calculating the right-hand side of Eq. (A.27), one obtains a change of 7.4% in the evaporation rate. In reality, the change will probably be even smaller, as can be obtained from more accurate calculation of evaporation rate based on kinetic theory analysis (Ytrehus, 1997; Shusser et al., 2000). This result justifies the assumption of constant evaporation rate in the unperturbed flow.

We now proceed to estimate droplet surface temperature perturbations. Writing the temperature as a sum of its base value T and its perturbation T' and linearizing, one obtains the following equation for T':

$$\frac{\partial T'}{\partial t} + v'_{\mathrm{r}-}\frac{\partial T}{\partial r} = D\nabla^2 T'. \tag{A.28}$$

We approximate the radial component of velocity perturbation in the liquid phase $v'_{\mathrm{r}-}$ as some average value that we shall write as

$$v'_{\mathrm{r}-} \approx \delta\frac{J}{\rho}, \tag{A.29}$$

where J/ρ is the characteristic velocity of the base flow and $\delta \ll 1$.

Then we can look for the solution for the temperature perturbation T' as a function of only r and t

$$\frac{\partial T'}{\partial t} = \frac{D}{r^2}\frac{\partial}{\partial r}\left(r^2\frac{\partial T'}{\partial r}\right) - \frac{\delta J}{\rho}\frac{\partial T}{\partial r}, \tag{A.30}$$

$$t = 0 \quad T' = 0, \tag{A.31}$$

$$r = 0 \quad T' \text{ is finite}, \tag{A.32}$$

$$r = R(t) \quad \frac{\partial T'}{\partial r} = -\frac{LJ'}{k}, \tag{A.33}$$

where J' is evaporation rate perturbation.

In the linear approximation

$$J' = \frac{\partial J}{\partial T}T'. \tag{A.34}$$

Then taking the variable Eq. (A.5), we obtain

$$\frac{\partial T'}{\partial t} + \left(\frac{2R}{r} - 1\right)\dot{R}\frac{\partial T'}{\partial y} = D\frac{R^4}{r^4}\frac{\partial^2 T'}{\partial y^2} + \frac{\delta J}{\rho}\frac{\partial T}{\partial y}, \tag{A.35}$$

$$t = 0 \quad T' = 0, \tag{A.36}$$

$$y = 0 \quad \frac{\partial T'}{\partial y} = hT', \tag{A.37}$$

$$y \to \infty \quad T' \text{ is finite},$$

where $\dot{R}$ is given by Eq. (A.12) and $h = \frac{L}{k}\frac{\partial J}{\partial T}$.

We have shown that the base solution $T(r, t)$ reaches its limit value for $t \to \infty$ very fast. Therefore, we approximate $\frac{\partial T}{\partial y}$ as its limit for $t \to \infty$. Using Eq. (A.22) one can show that

$$\lim_{t \to \infty} \frac{\partial T}{\partial y} = \frac{LJ}{k} e^{-\frac{J}{\rho D} y}. \tag{A.39}$$

Therefore assuming again a thin thermal boundary layer, we can state the following unsteady heat conduction problem for the temperature perturbation field inside the droplet

$$\frac{\partial T'}{\partial t} - \frac{J}{\rho}\frac{\partial T'}{\partial y} = D\frac{\partial^2 T'}{\partial y^2} + Q e^{-\frac{J}{\rho D} y}, \tag{A.40}$$

$$t = 0 \quad T' = 0, \tag{A.41}$$

$$y = 0 \quad \frac{\partial T'}{\partial y} = hT', \tag{A.42}$$

$$y \to \infty \quad T' \text{ is finite}, \tag{A.43}$$

where $Q = \delta \frac{LJ^2}{k\rho}$.

Using the Laplace transformation

$$v' = \int_0^\infty e^{-st} T' \, dt. \tag{A.44}$$

We obtain the following transformed problem

$$\frac{d^2 v'}{dy^2} + \frac{J}{\rho D}\frac{dv'}{dy} - \frac{sv'}{D} = -\frac{Q}{sD} e^{-\frac{J}{\rho D} y}, \tag{A.45}$$

$$y = 0 \quad \frac{\mathrm{d}v'}{\mathrm{d}y} = hv', \tag{A.46}$$

$$y \to \infty \quad v' \text{ is finite.} \tag{A.47}$$

The solution of Eqs. (A.45)–(A.47) is

$$v' = \frac{Q}{s^2} \mathrm{e}^{-\frac{J}{\rho D} y} \left[1 - \left(h + \frac{J}{\rho D} \right) \frac{e^{\frac{J}{2\rho D} y} e^{-y\sqrt{\frac{J^2}{4\rho^2 D^2} + \frac{s}{D}}}}{\left(\frac{J}{2\rho D} + \sqrt{\frac{J^2}{4\rho^2 D^2} + \frac{s}{D}} + h \right)} \right]. \tag{A.48}$$

Following the same method as for the unperturbed problem, it is possible after a rather lengthy computation to invert the transformation to obtain the following solution of Eqs. (A.40)–(A.43)

$$\begin{aligned} T' = {} & Qt\mathrm{e}^{-\frac{J}{\rho D} y} + \rho Q \left(h + \frac{J}{\rho D} \right) \\ & \times \left\{ \sqrt{\frac{Dt}{\pi}} \frac{\mathrm{e}^{-\frac{\left(y + \frac{J}{\rho} t \right)^2}{4Dt}}}{h(J + \rho Dh)} - \frac{1}{2Jh^2} \left[1 + h\left(y + \frac{J}{\rho} t \right) \right] \mathrm{erfc}\left(\frac{y}{2\sqrt{Dt}} + \frac{J}{2\rho} \sqrt{\frac{t}{D}} \right) \right. \\ & + \frac{\rho^2 D^2}{2J(J + \rho Dh)^2} \left[1 + \left(\frac{J}{\rho D} + h \right) \left(y - \frac{J}{\rho} t \right) \right] \mathrm{e}^{-\frac{J}{\rho D} y} \mathrm{erfc}\left(\frac{y}{2\sqrt{Dt}} - \frac{J}{2\rho} \sqrt{\frac{t}{D}} \right) \\ & \left. + \frac{(J + 2\rho Dh)}{2h^2 (J + \rho Dh)^2} \mathrm{e}^{hy + \left(\frac{J}{\rho D} + h \right) hDt} \mathrm{erfc}\left(\frac{y}{2\sqrt{Dt}} + \left(\frac{J}{2\rho} + hD \right) \sqrt{\frac{t}{D}} \right) \right\}. \end{aligned} \tag{A.49}$$

Then the surface temperature T'_s will be

$$T_s' = \frac{\rho^2 DQ}{J(J+\rho Dh)} + \rho Q\left(h + \frac{J}{\rho D}\right)$$

$$\times\left\{\sqrt{\frac{Dt}{\pi}}\frac{e^{-\frac{J^2}{4\rho^2 D}t}}{h(J+\rho Dh)} - \left[\frac{\rho^2 D^2}{2J(J+\rho Dh)^2} + \frac{1}{2Jh^2} - \frac{J}{2\rho h(J+\rho Dh)}t\right]\operatorname{erfc}\left(\frac{J}{2\rho}\sqrt{\frac{t}{D}}\right)\right. \quad \text{(A.50)}$$

$$\left. + \frac{(J+2\rho Dh)}{2h^2(J+\rho Dh)^2}e^{\left(\frac{J}{\rho D}+h\right)hDt}\operatorname{erfc}\left(\left(\frac{J}{2\rho}+hD\right)\sqrt{\frac{t}{D}}\right)\right\}.$$

As in the base problem, the characteristic time of the temperature change is much smaller than the time of the droplet evaporation and it is therefore possible to approximate T_s' by its limit value for $t \to \infty$. Substituting the expression for Q, we obtain

$$T_s' = \delta\frac{L}{c}\frac{J}{J+\rho Dh}. \quad \text{(A.51)}$$

We have obtained previously (Eq. (A.24)) that the change in the base surface temperature ΔT_s is

$$\Delta T_s = \frac{L}{c}. \quad \text{(A.52)}$$

Therefore

$$\frac{T_s'}{\Delta T_s} = \delta\frac{J}{J+\rho Dh} \ll 1. \quad \text{(A.53)}$$

One sees that the surface temperature perturbation is much smaller than any surface temperature change in the base flow. We have shown that the influence of the latter on the evaporation rate can be neglected with reasonable accuracy. Therefore, the influence of the surface temperature perturbation on the evaporation rate is completely negligible.

Appendix B. Stability of a highly superheated liquid droplet for large wave numbers

Comparison of our stability results with those for plane evaporating surfaces for large wave numbers n is limited by two factors. First, for an evaporating droplet, the surface curvature changes with time, as the droplet radius R decreases due to evaporation. Next, neglecting the terms of order $1/n^2$ makes the flow in the vapor irrotational, as can be seen from Eqs. (31)–(33). We will therefore compare our results with the analysis of the plane case only for irrotational vapor motion (Prosperetti and Plesset, 1984, p. 1600) and assume constant droplet radius R. The latter is possible, as for $n \to \infty$ the characteristic time of the perturbations is much smaller than that of the base flow (see Section 2.5).

Using the stability analysis of (Prosperetti and Plesset, 1984, p. 1600), one can retrieve that for irrotational flow in the vapor, steady temperature field in the base flow, low vapor density ($\rho_v \ll \rho$) and no gravitation, the evaporation of a plane liquid surface is unstable if

$$k < \frac{J^2}{\alpha\rho\sigma}. \tag{B.1}$$

Here k is the wave number for plane surface perturbations.

We now consider the evolution of the amplitude of the spherical liquid surface perturbation $a_1(t)$, which is governed by Eq. (41). Assuming $n \geq 1$ and $\alpha \ll 1$, one can write it as

$$\frac{R}{n}\frac{\mathrm{d}^2 a_1}{\mathrm{d}\tau^2} + 3\frac{\mathrm{d}a_1}{\mathrm{d}\tau} + \left(\frac{\sigma\rho n^2}{J^2 R} - \frac{n}{\alpha}\right)\frac{a_1}{R} = 0. \tag{B.2}$$

Here $\tau = Jt/\rho$.

Relating the perturbation wave numbers for the plane and the spherical cases, one can show that

$$n = kR. \tag{B.3}$$

Substituting in Eq. (B.2)

$$\frac{\mathrm{d}^2 a_1}{\mathrm{d}\tau^2} + 3k\frac{\mathrm{d}a_1}{\mathrm{d}\tau} + k^2\left(\frac{\sigma\rho k}{J^2} - \frac{1}{\alpha}\right)a_1 = 0. \tag{B.4}$$

Seeking the solution as

$$a_1 = \mathrm{e}^{\lambda\tau}, \tag{B.5}$$

we obtain two solutions

$$\lambda_1 = \frac{3k}{2}\left[-1 - \sqrt{1 + \frac{4}{9}\left(\frac{1}{\alpha} - \frac{\sigma\rho k}{J^2}\right)}\right], \tag{B.6}$$

$$\lambda_2 = \frac{3k}{2}\left[-1 + \sqrt{1 + \frac{4}{9}\left(\frac{1}{\alpha} - \frac{\sigma\rho k}{J^2}\right)}\right], \tag{B.7}$$

They have a positive real part only when

$$k < \frac{J^2}{\alpha\rho\sigma}. \tag{B.8}$$

Thus, we have obtained the same instability criteria for both plane Eq. (B.1) and spherical Eq. (B.8) cases.

Appendix C

The coefficients in Eq. (147) are

$$A(t)=\frac{R_1\left(1+\dfrac{R_1^{n+2}}{R_2^{n+2}}\right)\left(1-\dfrac{R_2^n}{R_1^n}\right)}{n\left(\dfrac{R_1^{n+2}}{R_2^{n+2}}-\dfrac{R_2^{n-1}}{R_1^{n-1}}\right)}+\frac{R_1\left(1-\dfrac{R_1^{n+1}}{R_2^{n+1}}\right)\left(1+\dfrac{R_2^{n-1}}{R_1^{n-1}}\right)}{(n+1)\left(\dfrac{R_1^{n+2}}{R_2^{n+2}}-\dfrac{R_2^{n-1}}{R_1^{n-1}}\right)}+\frac{\beta R_2}{n+1}-\frac{\alpha R_1}{n} \tag{C.1}$$

$$\begin{aligned}B(t)={}&\frac{R_1\left(1-\dfrac{R_2^n}{R_1^n}\right)}{n\left(\dfrac{R_1^{n+2}}{R_2^{n+2}}-\dfrac{R_2^{n-1}}{R_1^{n-1}}\right)}\\
&\times\Bigg\{(n+2)\frac{R_1^{n+1}\left(\dot R_1R_2-R_1\dot R_2\right)}{R_2^{n+3}}+\frac{2(1-\alpha)\dot R_1}{R_1}\left(\frac{R_1^3}{R_2^3}+\frac{R_1^{n+2}}{R_2^{n+2}}\right)-\frac{\left(1+\dfrac{R_1^{n+2}}{R_2^{n+2}}\right)}{\left(\dfrac{R_1^{n+2}}{R_2^{n+2}}-\dfrac{R_2^{n-1}}{R_1^{n-1}}\right)}\\
&\times\left[(n+2)\frac{R_1^{n+1}}{R_2^{n+3}}+(n-1)\frac{R_2^{n-2}}{R_1^n}\right]\left(\dot R_1\ R_2-R_1\dot R_2\right)\Bigg\}+\frac{\dot R_1\left(1+\dfrac{R_1^{n+2}}{R_2^{n+2}}\right)}{n\left(\dfrac{R_1^{n+2}}{R_2^{n+2}}-\dfrac{R_2^{n-1}}{R_1^{n-1}}\right)}\\
&\times\left[-(n-1)\left(1-\frac{R_2^n}{R_1^n}\right)+n(1-\alpha)\left(1-\frac{R_2^{n-3}}{R_1^{n-3}}\right)\right]+\frac{R_1\left(1-\dfrac{R_1^{n+1}}{R_2^{n+1}}\right)}{(n+1)\left(\dfrac{R_1^{n+2}}{R_2^{n+2}}-\dfrac{R_2^{n-1}}{R_1^{n-1}}\right)}\\
&\times\Bigg\{(n-1)\frac{R_2^{n-2}\left(\dot R_2R_1-R_2\dot R_1\right)}{R_1^n}+\frac{2(1-\alpha)\dot R_1}{R_1}\left(\frac{R_1^3}{R_2^3}+\frac{R_2^{n-1}}{R_1^{n-1}}\right)-\frac{\left(1+\dfrac{R_2^{n-1}}{R_1^{n-1}}\right)}{\left(\dfrac{R_1^{n+2}}{R_2^{n+2}}-\dfrac{R_2^{n-1}}{R_1^{n-1}}\right)}\end{aligned}$$

$$\times\left[(n+2)\frac{R_1^{n+1}}{R_2^{n+3}}+(=n-1)\frac{R_2^{n-2}}{R_1^{n}}\right]\left(\dot{R}_1\ R_2-R_1\dot{R}_2\right)\Bigg\}+\frac{\dot{R}_1\left(1+\frac{R_2^{n-1}}{R_1^{n-1}}\right)}{(n+1)\left(\frac{R_1^{n+2}}{R_2^{n+2}}-\frac{R_2^{n-1}}{R_1^{n-1}}\right)}$$

$$\times\left[(n+2)\left(1-\frac{R_1^{n+1}}{R_2^{n+1}}\right)-\ (n+1)(1-\alpha)\left(1-\frac{R_1^{n+4}}{R_2^{n+4}}\right)\right]-\frac{3\beta(1-\alpha)R_1^2\dot{R}_1}{(n+1)R_2^2}$$

$$+\frac{\alpha\dot{R}_1}{n\left(\frac{R_1^{n+2}}{R_2^{n+2}}-\frac{R_2^{n-1}}{R_1^{n-1}}\right)}\left[2n+1+\frac{(n-1)R_1^{n+2}}{R_2^{n+2}}+\frac{(n+2)R_2^{n-1}}{R_1^{n-1}}\right] \quad \text{(C.2)}$$

$$C(t)=\frac{2(1-\alpha)R_1\left(1-\frac{R_2^n}{R_1^n}\right)}{n\left(\frac{R_1^{n+2}}{R_2^{n+2}}-\frac{R_2^{n-1}}{R_1^{n-1}}\right)}$$

$$\times\Bigg\{\left(\frac{\ddot{R}_1}{R_1}-\frac{\dot{R}_1^2}{R_1^2}\right)\left(\frac{R_1^3}{R_2^3}+\frac{R_1^{n+2}}{R_2^{n+2}}\right)+\frac{\dot{R}_1R_1\left(\dot{R}_1R_2-R_1\dot{R}_2\right)}{R_2^4}\left(3+\frac{(n+2)R_1^{n-1}}{R_2^{n-1}}\right)$$

$$-\frac{\frac{\dot{R}_1}{R_1}\left(\frac{R_1^3}{R_2^3}+\frac{R_1^{n+2}}{R_2^{n+2}}\right)}{\left(\frac{R_1^{n+2}}{R_2^{n+2}}-\frac{R_2^{n-1}}{R_1^{n-1}}\right)}\left[(n+2)\frac{R_1^{n+1}}{R_2^{n+3}}+(n-1)\frac{R_2^{n-2}}{R_1^{n}}\right]\left(\dot{R}_1R_2-R_1\dot{R}_2\right)\Bigg\}$$

$$+\frac{\frac{2(1-\alpha)\dot{R}_1^2}{R_1}\left(\frac{R_1^3}{R_2^3}+\frac{R_1^{n+2}}{R_2^{n+2}}\right)}{n\left(\frac{R_1^{n+2}}{R_2^{n+2}}-\frac{R_2^{n-1}}{R_1^{n-1}}\right)}\left[n(1-\alpha)\left(1-\frac{R_2^{n-3}}{R_1^{n-3}}\right)-(n-1)\left(1-\frac{R_2^n}{R_1^n}\right)\right]$$

$$
\begin{aligned}
&+\frac{2(1-\alpha)R_1\left(1-\frac{R_1^{n+1}}{R_2^{n+1}}\right)}{(n+1)\left(\frac{R_1^{n+2}}{R_2^{n+2}}-\frac{R_2^{n-1}}{R_1^{n-1}}\right)}\left\{\left(\frac{\ddot{R}_1}{R_1}-\frac{\dot{R}_1^2}{R_1^2}\right)\left(\frac{R_1^3}{R_2^3}+\frac{R_2^{n-1}}{R_1^{n-1}}\right)+\frac{\dot{R}_1\left(\dot{R}_1R_2-R_1\dot{R}_2\right)}{R_1}\left(\frac{3R_1^2}{R_2^4}\right.\right.\\
&\left.\left.-\frac{(n-1)R_2^{n-2}}{R_1^n}\right)-\frac{\frac{\dot{R}_1}{R_1}\left(\frac{R_1^3}{R_2^3}+\frac{R_2^{n-1}}{R_1^{n-1}}\right)}{\left(\frac{R_1^{n+2}}{R_2^{n+2}}-\frac{R_2^{n-1}}{R_1^{n-1}}\right)}\times\left[(n+2)\frac{R_1^{n+1}}{R_2^{n+3}}+(n-1)\frac{R_2^{n-2}}{R_1^n}\right]\left(\dot{R}_1R_2-R_1\dot{R}_2\right)\right\}\\
&+\frac{\frac{2(1-\alpha)\dot{R}_1^2}{R_1}\left(\frac{R_1^3}{R_2^3}+\frac{R_2^{n-1}}{R_1^{n-1}}\right)}{(n+1)\left(\frac{R_1^{n+2}}{R_2^{n+2}}-\frac{R_2^{n-1}}{R_1^{n-1}}\right)}\\
&\times\left[(n+2)\left(1-\frac{R_1^{n+1}}{R_2^{n+1}}\right)-(n+1)(1-\alpha)\left(1-\frac{R_1^{n+4}}{R_2^{n+4}}\right)\right]+\frac{(1-\alpha)}{R_1}\left[\left(R_1\ddot{R}_1+2\dot{R}_1^2\right)\right.\\
&\left.\times\left(1+\frac{(1-\beta)R_1^2}{R_2^2}\right)-2(1-\alpha)\dot{R}_1^2\left(1+\frac{(1-\beta)R_1^5}{R_2^5}\right)\right]\\
&-\left[n(n+1)-2\right]\frac{\sigma}{\rho}\left(\frac{1}{R_1^2}-\frac{1}{R_2^2}\right)+\frac{2\beta(1-\alpha)R_1}{(n+1)R_2^5}\left(R_1\ddot{R}_1R_2^3+2R_0^3\dot{R}_1^2\right)\\
&+\frac{\alpha(1-\alpha)\dot{R}_1^2}{nR_1\left(\frac{R_1^{n+2}}{R_2^{n+2}}-\frac{R_2^{n-1}}{R_1^{n-1}}\right)}\left[2(2n+1)\frac{R_1^3}{R_2^3}+(n+1)(n+2)\frac{R_1^{n+2}}{R_2^{n+2}}-n(n-1)\frac{R_2^{n-1}}{R_1^{n-1}}\right]
\end{aligned}
\tag{C.3}
$$

References

Avedisian, C.T., 1985. Bubble growth in superheated liquid droplets. In: Cheremisinoff, N.P. (Ed.), Encyclopedia of Fluid Mechanics, vol. 3: Gas–liquid flows, pp. 130–190.

Birkhoff, G., 1954. Note on Taylor instability. Quart. Appl. Math. 12, 306–309.

Birkhoff, G., 1956. Stability of spherical bubbles. Quart. Appl. Math. 13, 451–453.

Carslow, H.S., Jaeger, J.C., 1959. Conduction of Heat in Solids. Oxford University Press, Oxford.
Chandrasekhar, S., 1961. Hydrodynamic and Hydromagnetic Stability. Clarendon Press, Oxford.
Chitavnis, S.M., 1987. Explosive vaporization of small droplets by a high-energy laser beam. J. Appl. Phys. 62, 4387–4393.
Drazin, P.G., Reid, W.H., 1981. Hydrodynamic Stability. Cambridge University Press, Cambridge.
Frost, D.L., 1989. Initiation of explosive boiling of a droplet with a shock wave. Exp. Fluids 8, 121–128.
Fuchs, H., Legge, H., 1979. Flow of a water jet into vacuum. Acta Astronautica 6, 1213–1226.
Higuera, F.J., 1987. The hydrodynamic stability of an evaporating liquid. Phys. Fluids 30, 679–686.
Hill, L.G., Sturtevant, B.S., 1990. An experimental study of evaporation waves in a superheated liquid. In: Meier, G.E.A., Thompson, P.A. (Eds.), Adiabatic Waves in Liquid–Vapor Systems. Springer-Verlag, New York, pp. 25–37.
Istratov, A.G., Librovich, V.B., 1969. On the stability of gas dynamics discontinuities associated with chemical reactions: the case of a spherical flame. Astronautica Acta 14, 453–467.
Kamke, E., 1944. Differentialgleichungen. Akademische Verlagsgesellschaft, Leipzig.
Lamb, H., 1932. Hydrodynamics. Cambridge University Press, Cambridge.
Landau, L.D., 1944. On the theory of slow combustion. Acta Phys.–Chim. USSR 19, 77 (also collected papers of L.D. Landau, Pergamon Press, pp. 396-403, 1965).
Lee, H.S., Merte, H., 1998. The origin of the dynamic growth of vapor bubbles related to vapor explosions. J. Heat Transfer 120, 174–182.
Mader, H.M., Zhang, Y., Phillips, J.C., Sparks, R.S.J., Sturtevant, B., Stolper, E., 1994. Experimental simulations of explosive degassing of magma. Nature 372, 85–88.
Mader, H.M., Phillips, J.C., Sparks, R.S.J., Sturtevant, B., 1996. Dynamics of explosive degassing of magma: observations of fragmenting two-phase flows. J. Geophys. Res. 101, 5547–5560.
Mader, H.M., Brodsky, E.E., Howard, D., Sturtevant, B., 1997. Laboratory simulations of sustained volcanic eruptions. Nature 388, 462–464.
McCann, H., Clarke, L.J., Masters, A.P., 1989. An experimental study of vapour growth at the superheat limit temperature. Int. J. Heat Mass Transfer 32, 1077–1093.
Meyer, J., Weihs, D., 1987. Capillary instability of an annular liquid jet. J. Fluid Mech. 179, 531–545.
Miller, C.A., 1973. Stability of moving surfaces in fluid systems with heat and mass transport. Part II: combined effects of transport and density differences between phases. AIChE J. 19, 909–915.
Miller, R.S., 1985. Photographic observation of bubble formation in flashing nozzle flow. J. Heat Transfer 107, 750–755.
Palmer, H.J., 1976. The hydrodynamic stability of rapidly evaporating liquids at reduced pressure. J. Fluid Mech. 75, 487–511.
Plesset, M.S., 1954. On the stability of fluid flows with spherical symmetry. J. Appl. Phys. 25, 96–98.
Plesset, M.S., Mitchell, T.P., 1956. On the stability of the spherical shape of a vapor cavity in a liquid. Quart. Appl. Math. 13, 419–430.
Plesset, M.S., Zwick, S.A., 1952. A nonsteady heat diffusion problem with spherical symmetry. J. Appl. Phys. 23, 95–98.
Prosperetti, A., 1977. Viscous effects on perturbed spherical flows. Quart. Appl. Math. 34, 339–352.
Prosperetti, A., Plesset, M.S., 1984. The stability of an evaporating liquid surface. Phys. Fluids 27, 1590–1602.
Reid, R., 1983. Rapid phase transitions from liquid to vapor. Advances in Chemical Engineering 12, 105–208.
Shepherd, J.E., Sturtevant, B., 1982. Rapid evaporation at the superheat limit. J. Fluid Mech. 121, 379–402.
Shusser, M., 1997. Theoretical investigation of the process of explosive boiling in droplets. D.Sc. Thesis. Technion — Israel Institute of Technology, Haifa.
Shusser, M., Weihs, D., 1999. Explosive boiling of a liquid droplet. Int. J. Multiphase Flow 25, 1561–1573.
Shusser, M., Ytrehus, T., Weihs, D., 2000. Kinetic theory analysis of explosive boiling of a liquid droplet, Fluid Dyn. Res., submitted.
Squire, H.B., 1953. Investigation of the instability of a moving liquid film. Brit. J. Appl. Phys. 4, 167–169.

Sturtevant, B., Shepherd, J.E., 1982. Evaporative instability at the superheat limit. Appl. Sci. Res. 38, 85–97.
Whittaker, E., Watson, G., 1927. A Course of Modern Analysis. Cambridge University Press, Cambridge.
Ytrehus, T., 1997. Molecular flow effects in evaporation and condensation at interfaces. Multiphase Science and Technology 9, 205–327.